Shared gene regulatory strategies for the p53 and ATF4-dependent transcriptional networks

Gabriele Baniulyte, Serene A. Durham, Lauren E. Merchant, Morgan A. Sammons

Department of Biological Sciences and The RNA Institute, University at Albany, State University of New York, Albany, NY, USA

Abstract

The master tumor suppressor p53 regulates multiple cell fate decisions, such as cell cycle arrest and apoptosis, via transcriptional control of a broad gene network. Dysfunction in the p53 network is common in a range of cancers, often through mutations that inactivate p53 or other members of the pathway. Induction of tumor-specific cell death by restoration of p53 activity without off-target effects has gained significant interest in the field. In this study, we explore the gene regulatory mechanisms underlying a putative anti-cancer strategy involving stimulation of the p53-independent Integrated Stress Response (ISR). Our data demonstrate that both the p53 and ISR pathways converge to independently regulate a common set of metabolic and pro-apoptotic genes. We investigated the architecture of multiple gene regulatory elements bound by p53 and the ISR effector ATF4 controlling this shared regulation. We identified additional key transcription factors that control basal and stress-induced regulation of these shared p53 and ATF4 target genes. Thus, our results provide significant new molecular and genetic insight into gene regulatory networks and transcription factors that are the target of numerous antitumor therapies.

Introduction

The global rewiring of cellular anabolic and catabolic processes that result from homeostatic changes include dynamic control of RNA and protein synthesis and turnover (Vihervaara et al., 2018; Advani and Ivanov, 2019). The DNA damage-inducible transcription factor, p53, directly activates transcription of a broad range of target genes involved in DNA repair, cell cycle arrest, and apoptosis. The well-described tumor suppressor function of p53 primarily relies on transcriptional activation of these target genes and their ability to mitigate the cellular and organismal consequences of damaged DNA. Nearly half of all human malignancies harbor mutations in p53 that facilitate and promote metastasis, tumorigenesis, and resistance to apoptosis (Zhu et al., 2015; Mantovani et al., 2019). These mutations generally lead to loss of DNA binding and an inability to transactivate canonical anti-proliferative p53 target genes (Bykov et al., 2018). Genotoxic chemotherapeutics, like doxorubicin and etoposide, are clinically relevant activators of wild-type p53, but the potential risk of resistance and secondary malignancies due to increased mutational burden remains a significant concern (Aziz et al., 2011). Given the powerful tumor suppression abilities of p53, restoration of the p53-regulated transcriptome without inducing additional DNA damage represents an intriguing approach for development of anticancer strategies and therapeutics.

Non-genotoxic, small molecule activation of the p53 pathway has been proposed as a potential solution. The first general approach involves small-molecule targeting of mutant p53 to either restore its wild-type function or prevent dominant-negative/gain-of-function activities (Yu et al., 2012; Chowdhury et al., 2014; Zhang et al., 2015; Bykov et al., 2018). A second approach uses compounds like the MDM2 inhibitor nutlin-3A to activate wild-type p53 in a non-genotoxic fashion, although early clinical trials suggest these approaches have limited efficacy when used alone (Andreeff et al., 2016; Kocik et al., 2019; Montesinos et al., 2020). A third approach involves bypassing p53 altogether via compounds that activate key anti-proliferative p53 targets in p53-deficient tumors (Hernandez Borrero et al., 2021; Tian et al., 2021). These compounds engage the Integrated Stress Response (ISR) network which is a well-studied effector of anti-proliferative and cell death gene expression programs. Interestingly, simultaneous ISR activation and MDM2 inhibition led to significant cell death and tumor regression not observed when the approaches were used individually (Andrysik et al., 2022), suggesting these pathways may work synergistically. These new ISR-stimulating approaches may be broadly applicable, as wild-type p53, p53-deficient, and p53 missense mutation-containing tumors could all be targeted. Thus, further exploration into the genetic and biochemical basis underlying this shared synergy between the p53 and ISR gene regulatory networks is needed for the design of more efficacious therapeutics and their mechanisms of action.

In this report, we identify shared gene targets and regulatory strategies of two distinct stress-dependent pathways, the p53 gene regulatory network (GRN) and the ATF4-dependent Integrated Stress Response (ISR) pathway. We demonstrate that an upstream enhancer element regulating the expression of *ATF3* is required for p53-dependent induction in response to

DNA damage, however, is not directly required for transcriptional induction of *ATF3* in response to ISR activating stimuli. ISR-dependent induction of *ATF3* requires ATF4 via binding and regulation of the *ATF3* promoter. We identified a second regulatory strategy whereby ATF4 and p53 target a shared enhancer to control *GADD45A,* another common gene target. Our data suggest that the p53 and ISR gene regulatory networks have shared gene targets and begin to unravel the DNA encoding and TF requirements for engagement of *cis*-regulatory elements that drive these behaviors.

Materials & Methods

Cell Culture and Treatments

The human colorectal cancer cell lines, HCT116 $TP53^{+/+}$ and HCT116 $TP53^{-/-}$, were cultured in McCoy's 5A Media (Corning, #10-050-CV) supplemented with 10% Fetal Bovine Serum (FBS) (Corning, #35-016-CV) and 1% Penicillin-Streptomycin (Gibco, #15240-062). Human mammary epithelial cells, MCF10A $TP53^{+/+}$ and MCF10A $TP53^{-/-}$ (Sigma-Aldrich) were cultured in 1:1 Dulbecco's Modified Eagle Medium: Ham's F-12 (Gibco, #11330-032) supplemented with 5% horse serum (Gibco, #16050-122), 20 ng/ml epidermal growth factor (Peprotech, #AF-100-15), 0.5 ng/ml hydrocortisone (Sigma, #H-0888), 100 ng/ml cholera toxin (Sigma, #C-8052), 10 µg/ml insulin (Sigma, #I-1882), and 1% Penicillin-Streptomycin (Gibco, #15240-062). The human near haploid cell line, HAP1 parental and HAP1 *ATF4*$^{-}$ cells (Horizon Genomics), were cultured in Iscove's Modified Dulbecco's Medium (Gibco, #12440-053) supplemented with 10% Fetal Bovine Serum (FBS) (Corning, #35-016-CV) and 1% Penicillin-Streptomycin (Gibco, #15240-062). All cell lines were cultured at 37°C and 5% CO_2 in a water-jacketed incubator.

For cell line treatments, cells were cultured for times indicated in each experimental figure/legend with either 5 µM nutlin-3A (Millipore Sigma, #45-SML0580) to stabilize p53 activation, 100 µM etoposide (Thermo Scientific, #J63651.MC), 2 µM tunicamycin (Thermo Scientific, #J62217.MA) or 2 mM histidinol (Acros Organics, #AC228831000). All drugs were freshly resuspended in DMSO and DMSO-only controls were added at equal volumes to each drug treatment.

Luciferase plasmid cloning and expression assays

Relevant plasmids and primers with cloning design are listed in Table S1. All cloning was done using NEBuilder (NEB, #E2621S). NanoLuciferase reporter plasmids were constructed using GADD45a_pHG plasmid as a backbone (kind gift from A. Fornace). pGB7 is the wild-type equivalent plasmid used throughout this study and includes *GADD45A* region chr1:67682954-67690203 with translationally fused nLuc. pGB7 also engineered to have PacI, Esp3I and MunI sites to facilitate removal of the 5' UTR and/or promoter region.

Luciferase assays were carried out using Nano-Glo® Dual-Luciferase® Reporter Assay System (#1620) following manufacturer's recommendations for 96 well plates. NanoLuciferase or firefly Luciferase values were normalized to constitutively expressed firefly luciferase (fLuc), or nanoLuciferase (nLuc) levels that were generated by co-transfected pGL4.53 or pNL1.1 (Promega, #E5011, #N1441) plasmids, respectively.

Lentivirus production, purification and transduction

All lentiviral particles were packaged using HEK293FT cells seeded at a density of 250,000 cells per well in 6-well culture plates. In brief, 1 µg of pLKO.1-Puro TRC plasmid containing either non-targeting shRNA (5'-CAACAAGATGAAGAGCACCAA-3') or ATF4-targeted shRNA (5'-GCCTAGGTCTCTTAGATGATT-3') was combined with 1 µg of packaging plasmids psPAX2 and pMD2.G, mixed at a molar ratio of 2:1. The plasmid mix was diluted in jetPRIME buffer (Polyplus Transfection, 89129-924) and transfection reagent, following the manufacturer's protocol. pMD2.G was a gift from Didier Trono (Addgene plasmid # 12259). psPAX2 was a gift from Didier Trono (Addgene plasmid # 12260). Lentivirus-containing supernatants were collected at 24 and 48 h post-transfection and filtered through 0.45-µm nitrocellulose filters and stored in aliquots at −80 °C. Cells were transduced with lentiviral supernatant supplemented with 8 µg/ml Polybrene (hexadimethrine bromide). After 24 hours, cells were selected for viral infection via addition of 2 µg/mL final of puromycin for 72 hours.

Quantitative Real Time PCR (RT-qPCR)

Total RNA was isolated (Quick RNA miniprep, Zymo, #R1055) with an on-column treatment of 50U of DNase I for 30 minutes. Single-stranded cDNA was generated (High Capacity cDNA Reverse Transcription Kit, ABI #4368814) and qPCR was performed using the relative standard curve method and iTaq Universal SYBR Green Supermix reagents (BioRad). All RT-qPCR primers are presented in Table S1.

Western Blotting

Total protein was isolated using a custom RIPA buffer (50mM Tris-HCl[pH 7.4], 150mM NaCl, 1% NP-40, 0.5% sodium deoxycholate, 0.1% SDS) supplemented with protease/phosphatase inhibitors (Pierce, 78442). Protein concentration was measured using the BCA approach (Pierce, 23227), and equal protein

concentrations were analyzed using the ProteinSimple® Wes platform with the 12–230 kDa Wes Separation Module containing 8 × 25 capillary cartridges per manufacturer's instructions. Specific antibodies used were: anti-p53 (clone DO-1, BD Bioscience #554293), anti-ATF3 (Abcam, #AB207434), anti-ATF4 (Cell Signaling, #D4B8), anti-GADPDH (Cell Signaling, #5174S).

CUT&RUN

$1.5x10^6$ cells per CUT&RUN reaction were prepared for batch processing using the Epichyper CUTANA™ CUT&RUN protocol v1.9 and reagents (Epicypher, #14-1048). Briefly, cells bound to activated Concanavalin A beads were incubated overnight with 0.5 µg of either anti-ATF4 antibody or non-specific rabbit IgG. DNA fragments were purified using phenol/chloroform extraction and 20 ng of purified DNA was used to construct an Illumina-compatible sequencing library (Liu, 2019) which was optimized for CUT&RUN-sized DNA fragments and NEBNext Ultra II DNA Library reagents (NEB #E7660). Library concentrations were quantified (NEBNext Library Quant Kit for Illumina, E7630), pooled at equimolar concentrations, and sequenced in paired-end mode on the Illumina NextSeq 2000 at the University at Albany Center for Functional Genomics.

CUT&RUN and ChIP-seq Data Analysis

Raw paired-end sequencing reads for CUT&RUN were aligned to the hg38 human genome reference using hisat2 (Kim et al., 2019) with the following options (-X 700 -I 10 --no-spliced-alignment). ChIP-seq reads (Andrysik et al., 2017) for HCT116 input (GSM2296270), p53 ChIP-seq under DMSO-treatment (GSM2296271), and p53 ChIP-seq under Nutlin-3A-treatment (GSM2296272) were downloaded from Gene Expression Omnibus and aligned to the hg38 human genome reference using hisat2. BigWig files for visualization were produced via deepTools (Ramírez et al., 2016).

RNA Sequencing

Cells were treated with either DMSO, nutlin-3A, etoposide, tunicamycin, or histidinol as described above in a six-well plate for 6h and total RNA was isolated (Quick RNA miniprep, Zymo, #R1055). PolyA+ RNA was purified using Dynabeads Oligo $(dt)_{25}$ (Invitrogen, #61012) and fragmented at 94°C for 15 min. Fragmented RNA was used as the template for double-stranded cDNA production which was then used to construct an Illumina-compatible sequencing library (NEBNext Ultra II Directional RNA Library Kit for Illumina, NEB E7760). Libraries were quantified using qPCR (NEBNext Library Quantification Kit, NEB E7630) and an Agilent Bioanalyzer and then pooled for sequencing on an Illumina NextSeq 2000 at the University at Albany Center for Functional Genomics or on an Illumina Hiseq 2000 at Azenta/GeneWiz. Transcript abundance from the ENSEMBL hg38 genome assembly (v.104) was quantified using *kallisto* in bootstrap mode (*kallisto* quant -b 100) (Bray et al., 2016). Resulting transcript counts (TPM) were imported and processed via tximport (Soneson et al., 2015) and differential expression was quantified using DESeq2 (Love et al., 2014). Pathway enrichment analyses for differentially expressed genes were performed using enrichr (Chen et al., 2013; Kuleshov et al., 2016; Xie et al., 2021).

STARRSeq enhancer mutagenesis screen

STARRSeq library preparation was done following a published protocol (Neumayr et al., 2019) with minor modifications as described here. To simplify STARRSeq library preparation, hSTARR-seq_ORI vector (Addgene #99296) (Muerdter et al., 2018) was modified by adding partial Illumina P5 and P7 adaptor sequence before AgeI and after SalI restriction sites, respectively, yielding plasmid pGB118. Mutagenesis library was constructed as a 250 nt of *GADD45A* intronic enhancer region (chr1:67686701-67686950) with a 'N' mixed base or a deletion at every position and 25 nt pGB118 matching overhangs on the 5' and 3' ends. The library was ordered as an oligo pool (oPool, IDT). oPool library was amplified for 10 cycles with primers SL1947 + SL1948 and cloned into pGB118 cut with AgeI and SalI using NEBuilder (NEB, #E2621S). 18 million HCT116 $TP53^{+/+}$ or $TP53^{-/-}$ cells were transfected with 10 µg STARRSeq mutagenesis plasmid library using JetPrime Transfection Reagent. 5h after transfection, the media was replaced with fresh media supplemented with 0.001% DMSO, 5 µM nutlin-3A or 2 µM Tunicamycin. RNA was extracted 6h post-treatment. Processed RNA and plasmid DNA libraries were sequenced Illumina NextSeq 2000 at the University at Albany Center for Functional Genomics as 2x150 paired-reads. R1 and R2 reads were first merged using bbmerge tool from BBMap (Bushnell et al., 2017). Merged reads were then collected and counted using a strict string pattern matching the expected library sequences. Relative expression was calculated as an RNA/DNA ratio.

Data Availability

Datasets are available at Gene Expression Omnibus (GEO) under accession numbers GSE211244 (RNAseq), GSE211264 (CUT&RUN), GSE226617 (STARRSeq mutagenesis screen).

Results

ATF3 is induced by the Integrated Stress Response (ISR) in a p53-independent manner.

Activating Transcription Factor 3 (*ATF3)* is an immediate-early response gene acting as a hub of the cellular adaptive-response network. *ATF3* mRNA is upregulated in response to numerous cellular stresses including both DNA damage and endoplasmic reticulum (ER) stress (Hai et al., 1999; Hashimoto et al., 2002; Jiang et al., 2004; Hai, 2006; Lu et al., 2006). Recent reports suggest that activation of the ISR leads to induction of p53 target genes, including *ATF3*, but the specific transcription factor requirements for this behavior have not been fully characterized. To this end, we investigated whether p53 was specifically required for ATF3 induction under DNA damage and ISR conditions. We first confirmed that *ATF3* mRNA expression could be induced by both p53 and ISR pathways via quantitative reverse transcription polymerase chain reaction (RT-qPCR) in the isogenic human colorectal carcinoma cell lines, HCT116 *TP53*+/+ (p53 WT) or *TP53*-/- (p53 null). We used two independent means to activate the p53 and ISR pathways. Etoposide activates several transcription factors, including p53, via induction of DNA double strand breaks (DSBs) (van Maanen et al., 1988; Shieh et al., 1997). Nutlin-3A specifically inhibits the negative p53 regulator, MDM2, leading to highly specific stabilization and activation of p53 in a non-genotoxic manner (Vassilev et al., 2004). In vertebrates, the ISR is activated by stimuli that induce ER stress, nutrient and heme deprivation, and viral infection (Taniuchi et al., 2016). Therefore, we treated our HCT116 cell lines with tunicamycin, an inhibitor of N-linked glycosylation which induces ER stress by causing an accumulation of unfolded proteins in the ER (Ding et al., 2007), or histidinol, which initiates the amino acid response (AAR) via depletion of the essential amino acid, histidine (Fu and Kilberg, 2013).

We first confirmed the specificity of these chemical treatments via examination of p53 protein abundance and expression of canonical p53 and ISR target genes *CDKN1A/*p21 and the asparagine synthetase *ASNS* (el-Deiry et al., 1993; Szak et al., 2001; Siu et al., 2002). p53 protein abundance (Fig. 1B) and *CDKN1A/*p21 mRNA (Fig. 1D) expression increased in response to both etoposide and nutlin-3A in a p53-dependent manner but did not increase in response to ISR activation by tunicamycin or histidinol. Both ER stress and AA starvation led to *ASNS* induction in a p53-independent. Neither Nutlin-3A nor etoposide treatments altered *ASNS* mRNA abundance in either genetic background, suggesting the ISR is not activated after DNA DSB induction. Taken together, these two results suggest that tunicamycin- and histidinol-mediated induction of the ISR in HCT116 cells does not require p53 activity (Fig. 1D, E). Although the induction of *ASNS* mRNA under ISR stimulating conditions relative to DMSO vehicle control was not dependent on p53, we note that the total abundance of *ASNS* mRNA is slightly reduced in HCT116 p53 null cell line.

ATF3 mRNA and protein levels increased in response to both p53 and ISR stimulating treatments in HCT116 WT cells (Fig. 1A, C). p53 is required for induction of ATF3 mRNA in response to nutlin-3A and etoposide, whereas ATF3 protein is still induced in response to etoposide in the absence of p53. Total ATF3 protein abundance is considerably lower in HCT116 p53 null cells relative to HCT116 WT suggesting that p53 activity is required for basal, but not induced, ATF3 expression. Importantly, ATF3 mRNA and protein induction are p53-independent in response to both tunicamycin and histidinol. Coupled with the lack of p53 stabilization and *CDKN1A/p21* induction, these data suggest that upregulation of *ATF3* in response to ISR does not require p53 (Fig. 1A, C).

ATF4 and p53 independently regulate expression of *ATF3*

Our results suggest that both p53 and the ISR regulate *ATF3* transcription in a parallel, potentially redundant fashion. *ATF3* induction during the DNA Damage Response (DDR) is largely p53-dependent in HCT116 cells (Fig. 1A, C); however, the induction of *ATF3* mRNA in response to activation of the ISR occurs in the absence of p53 (Fig.1A, C). ATF4, a member of the basic region-leucine zipper (bZIP) superfamily of stress-dependent TFs, is one of the main effectors of the ISR and a critical regulator of the transcription downstream of ISR activation (Chen et al., 1996; Han et al., 2013). Prior work suggests that ATF4 regulates the expression of *ATF3* in other cellular contexts, therefore we tested whether ATF4 activity might underlie the p53-independent induction of *ATF3* mRNA expression in response to ER stress and AA starvation (Pan et al., 2007; Kilberg et al., 2009; Fu and Kilberg, 2013). We first characterized the activity of *ATF4* in response to ISR-activating stimuli in our HCT116 p53 WT and p53 null cells to confirm ISR-dependent ATF4 expression. As expected, *ATF4* mRNA and protein levels increase in response to both ER stress (via tunicamycin treatment) and AA starvation (via histidinol treatment), whereas *ATF4* mRNA and protein expression were unaffected in response to p53 stabilization (via Nutlin-3A treatment) or DNA damage (via etoposide treatment) (Fig. 2A, D).

To determine the role of ATF4 in regulating *ATF3* induction downstream of ISR activation, we created HCT116 p53 WT and p53 null cells expressing either a non-targeting control (scramble) or an *ATF4*-directed shRNA. *ATF4* mRNA and protein abundance is substantially reduced in *ATF4* shRNA-expressing cell lines compared to those expressing the non-targeting shRNA control (Scramble) (Fig. 2B, E). *ASNS* mRNA abundance was significantly reduced after knockdown of ATF4, demonstrating the effectiveness of these reagents in ablating both ATF4 expression and activity under basal and ISR-activating conditions (Fig. 2G). *ATF3* induction in response to etoposide was unaffected after ATF4 knockdown (Fig. 2I). Conversely, knockdown of ATF4 significantly reduced the amount of *ATF3* mRNA induction in response to ER stress, suggesting a direct role for ATF4 activity in mediating ISR-dependent *ATF3* expression (Fig. 2I). We extended our analysis to isogenic *ATF4*+ (HAP1 parental) and *ATF4*- (HAP1 ATF4KO) haploid leukemia cell lines. HAP1 ATF4KO cells lack detectable levels of *ATF4* mRNA and protein under basal conditions and in response to ER stress (Fig. 2C, F). Deletion of ATF4 led to a complete ablation of both *ASNS* and *ATF3* mRNA induction in response to ER stress, confirming that *ATF3* induction in response to ISR is ATF4-dependent (Fig. 2H, J). These results demonstrate that ATF4 acts as the main effector of *ATF3* induction downstream of ISR activation in response to ER stress and AA deprivation and that p53 primarily mediates *ATF3* transcription after DNA damage.

ATF4 and p53 occupy distinct regulatory regions in the *ATF3* gene locus

Our results demonstrate a genetic dependence for p53-mediated activation of *ATF3* transcription under DNA damage conditions, and a functionally distinct, ATF4-dependent pathway that regulates *ATF3* transcription during the ISR. In order to understand whether this regulation occurs via direct binding to regulatory regions controlling *ATF3*, we generated novel cleavage under targets & release under nuclease (CUT&RUN) (Skene and Henikoff, 2017) genomic binding data for ATF4. HCT116 cells were treated with either DMSO (control), p53-activating (etoposide), or ISR-stimulating agents (tunicamycin or histidinol) for 6h and then subjected to CUT&RUN using either an ATF4-specific antibody or a non-specific IgG isotype control. Three biological replicates were generated for each treatment condition. Regions of significant ATF4 enrichment (relative to IgG control signal) were identified using *macs2* (Zhang et al., 2008). We first created a set of high-confidence, ISR-activated ATF4 binding events by considering only peaks called from 5 out of 6 experiments from cells treated with either tunicamycin or histidinol (Fig. S1A-C). The rationale for filtering peaks in this manner is to allow examination and further analysis of putative ATF4 binding events that are universal to the ISR, while also accounting for potential variability within individual biological replicates or treatment conditions. In support of this approach, we observe 7,723 ATF4 binding events shared across five out of six experimental conditions, with 5,093 (65%) existing across all observations. These 7,723 peaks were then examined for expected features of ATF4 binding, including specificity during ISR stimulation and enrichment of predicted ATF4 DNA binding motifs.

Known motif enrichment analysis revealed the predicted ATF4 motif as the most highly-enriched in the high-confidence peak set, followed by enrichment of motifs for the known heterodimer partner, C/EBP homologous protein (CHOP) (Fig. 3A). Similar enrichment of a motif most closely matching the known ATF4 motif was observed using *de novo* motif enrichment strategies on the high-confidence set (Fig. 3B). Enrichment of CUT&RUN sequencing tags was highly specific for tunicamycin and histidinol treatment conditions compared to either vehicle (DMSO) control or under DNA damage (etoposide) conditions (Fig. 3C). We first confirmed previous reports from literature which suggest the transcriptional activation of *ASNS* in response to ISR stimuli is mediated via binding of ATF4 to the promoter region of this gene in response to AA starvation (Chen et al., 2004). Our CUT&RUN analysis reveals a significant, ISR-specific enrichment of ATF4 at the *ASNS* promoter in response to both AA starvation and ER stress (Fig. S1D). These data suggest that our set of high-confidence, ISR-dependent ATF4 peaks are likely representative of true ATF4 genomic binding events. Therefore, we used this set of genomic locations engaged by ISR-activated ATF4, along with previously published p53 ChIP-seq data (Andrysik et al., 2017), to identify putative ATF4 and p53 binding events that might directly regulate *ATF3* transcription. We observe an ATF4 binding event within a DNAse-hypersensitive site (DHS) overlapping the first exon/transcriptional start site (TSS) of *ATF3* in response to both ER stress and amino acid deprivation, but not during the DDR or in vehicle-treated control conditions (Fig. 3D). This region corresponds with a previously reported promoter region regulating ISR-dependent *ATF3* transcription (Fu and Kilberg, 2013). p53, on the other hand, binds to a DHS approximately 13 kb upstream (p53-bound DHS) from the ATF4-bound *ATF3* promoter. ATF4 also occupies a spatially distinct DHS 15kb upstream (ATF4-bound DHS) from the *ATF3* TSS in an ISR-

dependent fashion. These novel biochemical binding datasets for ATF4 binding to the genome in response to DNA damage and ISR activation further suggest a direct role for ATF4 in regulation of ISR-dependent *ATF3* and confirm the ATF4-independence of *ATF3* transcription downstream of DNA damage.

Analysis of the regulatory elements controlling stress-dependent *ATF3* expression

Biochemical analyses and genetic loss-of-function experiments confirm that p53 and ATF4 likely regulate expression of *ATF3* independent of each other (Figs. 1-3). To determine if the two distinct upstream DHS bound by p53 or ATF4 were contributing to transcriptional activity of *ATF3* in response to stress, we tested their ability to activate transcription of a luciferase reporter gene via a minimal promoter (minP). The upstream ATF4-bound DHS does not act as an enhancer, as there was no significant difference in the levels of transcription driven from this site when compared to those driven by the negative control (minP), under any of the conditions and cellular contexts tested (Fig. 4A). The p53-bound DHS drove substantial transcriptional activity under basal conditions with a significant increase in activity upon Nutlin-3A treatment. Basal and p53-induced activity of this element were significantly reduced when the putative p53 binding motif was mutated or when assayed in HCT116 p53 null cell lines. Loss of p53 does not completely ablate basal transcriptional activation suggesting other transcription factors likely contribute to basal, unstimulated *ATF3* activity. However, no additional transcriptional activation by the p53-bound DHS was observed in response to tunicamycin (Fig. 4A). Taken together, these data suggest that the p53-bound DHS likely regulates *ATF3* transcription under basal and conditions that stabilize p53, and that the adjacent ATF4-bound DHS likely does not facilitate ISR-mediated *ATF3* transcription.

Prior work suggests that ATF4 regulates *ATF3* via interaction with two canonical ATF/CREB family motifs within the *ATF3* promoter in hepatocarcinoma (HepG2) cells in response to ISR activation (Fu and Kilberg, 2013). This regulation depends on both a CRE site (nt −93/−85, TGACGTCA) existing upstream of a CARE site (nt −23/−15, TGATGXAAX) within the *ATF3* gene promoter (−107/+35) (Weidenfeld-Baranboim et al., 2009; Hai et al., 2010). We thus assessed whether ATF4 might regulate *ATF3* via interaction with these elements, as ISR-induced ATF4 binding to an upstream DHS had no effect on *ATF3* transcription. We thus tested the activity of luciferase reporters driven by the −107/+35 promoter fragment of the ATF3 gene - containing both the CARE and CRE sequences (WT ATF3 promoter), as well as constructs containing mutations in one (CARE and CRE) or both (CARE/CRE) of these sites, in control and ATF4-deficient HAP1 cell lines. Consistent with prior reports, both ER stress (tunicamycin) and AA starvation (histidinol) treatments led to increased transcription driven by the WT *ATF3* promoter construct in an ATF4-dependent manner (Fig. 4B). Mutation of the CARE and CRE sites, both capable of supporting ATF4 binding, showed significantly and substantially reduced ability to drive both basal and ISR-induced transcription. Our data are also consistent with the prior observation that the CARE site is required for amino acid starvation-induced activity, but is dispensable for ER stress-induced transcription (Pan et al., 2007; Fu and Kilberg, 2013). Similar to our results for the upstream p53-bound DHS, these data suggest that multiple transcription factors in addition to p53 and ATF4 are likely involved in the basal and stress-dependent regulation of *ATF3*, consistent with models whereby multiple transcription factors work in a context-dependent and often combinatorial manner to drive transcription (Smith et al., 2013; Chaudhari and Cohen, 2018; Zeitlinger, 2020; Choi et al., 2021; Kim et al., 2021). Our data using genetic depletion strategies, biochemical binding assays, and testing putative *cis*-regulatory element activity using reporter gene assays data provide evidence for a model whereby activation of *ATF3* transcription in response to DNA damage and the ISR occurs through distinct transcription factors binding to distinct regulatory elements.

ISR-mediated induction of *ATF3* does not require the upstream enhancer bound by p53

ATF4 and p53 likely independently regulate expression of *ATF3* and occupy distinct putative regulatory regions in a stress-dependent manner (Figs. 2I, 3D). Our *in vitro* reporter assays provide direct evidence for stress-specific roles of ATF4 and p53 at specific *cis*-regulatory elements of *ATF3* (Figure 4A-B). To further characterize the mutual independence of p53 and ATF4 and to demonstrate whether these binding events control *ATF3* transcription *in vivo*, we utilized a CRISPR interference (CRISPRi) system to block effector protein binding at specific regulatory elements (Gilbert et al., 2013; Qi et al., 2013). We chose the dCas9-KRAB CRISPRi system which fuses the catalytically inactive form of *Streptococcus pyogenes* Cas9 with a KRAB transcriptional repressor domain (Margolin et al., 1994). dCas9-KRAB targeting to cis-regulatory elements has proven an effective strategy for blocking effector protein binding and inhibiting regulatory elements and linked gene expression (Thakore et al.,

2015; Yeo et al., 2018; Catizone et al., 2020). We first targeted dCas9-KRAB to the *ATF3* promoter as proof of principle, since repression of a gene promoter should inhibit transcription initiated from that element. Targeting of dCas9-KRAB to the putative *ATF3* promoter, approximately 100 bp upstream of the TSS (Fig. 4D) significantly reduced *ATF3* mRNA levels compared to all three off-target controls (FGF2 enhancer, 5' control, and 3' control) (Fig. 4C). This repression was observed under basal (DMSO), DNA damage, and ER stress conditions, demonstrating the effectiveness of using the CRISPRi system to inhibit transcription of *ATF3* via specific targeting of regulatory elements. Targeting dCas9-KRAB to the p53-bound enhancer significantly reduced *ATF3* mRNA levels in response to basal and etoposide-treated conditions when compared to all non-targeting controls (Fig. 4D). Targeting of dCas9-KRAB to any of the three control locations did not significantly alter either basal or DNA damage-induced *ATF3* expression (Fig. 4D). The canonical ISR and p53-dependent gene targets *ASNS* and *CDKN1A/*p21 were unaffected by targeting dCas9-KRAB to the p53-bound enhancer or control regions (Figs. 4E, F). Induction of *ATF3* mRNA in response to tunicamycin-induced ER stress was not affected when targeting the p53-bound enhancer (Fig. 4D). These results indicate that while this p53-bound upstream enhancer region is important for both basal and p53-mediated transcriptional activation of *ATF3*, it is not directly required for the induction of *ATF3* in response to ER stress.

Global transcriptome analysis identifies common gene regulatory targets of the p53 and Integrated Stress Response

Our data demonstrate that the DNA damage response (via p53) and the Integrated Stress Response (via ATF4) both activate transcription of *ATF3,* although they do so independently of one another through at least two different gene regulatory elements. We sought to determine if this parallel stress-dependent target gene activation by the p53 and ISR pathways may be more widespread. We thus performed polyA+ RNA-seq on HCT116 p53 WT and p53 null cells after 6 hours of treatment with p53 or ISR-activating stimuli: DMSO (vehicle), 5 μM Nutlin-3A,100 μM etoposide, 2 μM Tunicamycin, or 2 mM histidinol. Three biological replicates were analyzed for each treatment condition via transcript counting (*kallisto*, 100 bootstraps) (Bray et al., 2016) and differential gene expression analysis (*deseq2)* (Love et al., 2014). We confirmed that each treatment was effective in eliciting an expected transcriptional response by performing gene ontology analysis of the genes upregulated (Fig. S2A-D) and downregulated (Fig. S2E-H) when compared to vehicle control in HCT116 WT cells (Chen et al., 2013; Kim et al., 2019; Xie et al., 2021). Treatment with either nutlin-3A or etoposide led to significant upregulation of genes and gene categories consistent with a functional p53 response, including those related to known p53 signaling and the cellular response to DNA damage (Fig. S2A-B). Treatment with tunicamycin led to upregulation of genes consistent with ER stress and transcriptional regulation (Fig. S2C) and downregulation of genes involved in translation and ribosome biogenesis (Fig. S2G). Similar ontology groups were enriched in differentially regulated genes after treatment with histidinol (Fig. S2D,H), although we note expected treatment specific enrichment of ER stress-associated genes after tunicamycin treatment and metabolic regulation after histidinol addition. Taken together, these broad analyses of gene regulation via standard gene ontology methods demonstrate that each chemical treatment recapitulates expected cellular responses to specific cell stress conditions.

We next established parameters to define genes that are regulated in a similar fashion as *ATF3* in response to p53 and ISR activation. These genes would be i) significantly upregulated in response to both p53- and ISR-activating stimuli in HCT116 p53 WT cells relative to DMSO, ii) p53-dependent in response to nutlin-3A treatment, a stimuli that specifically activates and stabilizes p53 (Fig. S2I), and iii) significantly upregulated in the absence of p53 in response to ISR-activating treatments, tunicamycin and histidinol. The inclusion of nutlin-3A-mediated regulation strictly limits our gene set to those genes regulated by p53 directly, as opposed to via DNA damage-dependent, but p53-independent mechanisms, as we have previously observed (Catizone et al., 2020). Ultimately, these criteria yielded 27 genes upregulated in response to p53 activation, ER stress, and AA starvation (Fig. 5A). As expected, *ATF3* was in this gene set upregulated in response to all four treatment conditions relative to DMSO, providing support for selection criteria and the quality of the data set (Fig. 5B-C). Gene ontology analysis of this set of 27 genes suggests a shared involvement in regulation of apoptotic signaling pathways and transcription by RNA polymerase II. We also observed regulation of the mitogen-activated protein kinase (MAPK) signaling cascade, a pathway known to integrate and amplify signals from a diverse range of stimuli to produce an appropriate cellular response (Zhang and Dong, 2007; Chavel et al., 2010) (Fig. 5D). Similar pathway analysis on the shared downregulated genes reveal shared function in protein synthesis, potentially reflecting a cellular switch from

an anabolic to catabolic state, consistent with prior reports of broad translational control by these pathways (Fig. 5E) (Loayza-Puch et al., 2013; Zaccara et al., 2014; Andrysik et al., 2017; Tameire et al., 2019; Tian et al., 2021).

We next analyzed the behavior of these commonly upregulated genes in HCT116 p53 null cells to determine whether their induction is truly p53-dependent or independent in response to ISR-inducing stimuli. Interestingly, although 11 of the 27 commonly upregulated genes behave similarly to *ATF3* (Figs. 5B,C), the remaining genes show some dependence on p53 for full activation downstream of the ISR. p53 protein levels are not stabilized in response to ISR-activating stimuli (Fig. 1B) and we observe no evidence that canonical p53 target genes like *CDKN1A*/p21 respond to ISR-activating stimuli (Fig. 1D), suggesting that this partial dependence on p53 is likely due to indirect activity of p53 in regulating other activators within the ISR. Consistent with this possibility, we note diminished ATF4 protein levels in the absence of p53 in both basal and ISR-induced conditions (Fig. 2A). While additional work is required to determine the causal relationship, if any, between loss of p53, reduced ATF4 protein abundance, and the effect on ISR-dependent gene expression, our data suggest that p53 and ATF4-dependent transcriptional control mechanisms are likely to be functionally independent.

Lastly, we validated the p53 and ATF4-dependence of a select set of these target genes using a battery of cell lines and genotypes. We first examined p53-dependence for three of the candidate genes regulated similarly to *ATF3, GADD45A* (Zhan et al., 1994; Ebert et al., 2019)*, SESN2* (Budanov and Karin, 2008; Garaeva et al., 2016)*,* and *GDF15* (Osada et al., 2007; Li et al., 2021). We tested the behavior of these three genes in response to etoposide or tunicamycin treatment in p53 WT and p53 null HCT116 (Fig. 6A-D) and MCF10A mammary epithelial lines (Fig. 6E-H). Each gene was induced by both treatments and etoposide-mediated induction required an intact p53 response. Conversely, p53 was not required for induction of these genes in response to tunicamycin, consistent with the parallel nature of the p53 and ATF4-dependent transcriptional networks. These data in MCF10A cell lines also demonstrate that this behavior is not limited to colon carcinoma cell lines. We extended this analysis by examining the behavior of these gene targets in either HAP1 parental or *ATF4*-cell lines. *ATF4* activity is required for induction of three of these gene targets in response to tunicamycin (Fig. 6I-L). Nutlin-3A treatment, which is highly specific for activation of p53, fails to induce expression of *ATF3, GADD45A, SESN2,* and *GDF15* likely due to the previously identified loss-of-function *TP53* S215G variant allele (Moder et al., 2017) present in these cell lines. The absence of p53 and the presence of a functional ISR further suggest the functional independence of these pathways. Taken together, our data identify a set of "dual response" genes that are independently regulated by p53 or ATF4 in response to specific stress conditions.

GADD45A gene-derived reporter system for assessing DDR and ISR enhancers

Our data demonstrate that p53 activates *ATF3* transcription via an upstream, distal enhancer element, whereas we confirmed prior observations that ATF4 binds to and regulates transcription via the *ATF3* proximal promoter. We sought to extend these observations to determine whether any additional "dual response" genes have *cis*-regulatory strategies similar to *ATF3*. We focused our analysis on the gene target *GADD45A*. *GADD45A* was previously reported to contain a p53-bound enhancer element located within the 3rd intron (Zhan et al., 1998; Daino et al., 2006). Our CUT&RUN analysis of ATF4 genomic binding under ISR-stimulating conditions suggests ATF4 also binds to this putative regulatory element (Fig. 7A). We thus tested whether p53 and ATF4 binding to this element controls *GADD45A* mRNA transcription under p53 or ISR activating conditions, respectively, utilizing a newly constructed luciferase reporter system (Fig. 7B). We reasoned that (1) GADD45A is relatively small (~3 kb) therefore it is convenient for plasmid-based genetic manipulations, and that (2) this reporter might be more relevant for stress-dependent promoter-enhancer interaction studies as an almost native genetic context, including enhancer:promoter distance and location, is maintained. We tested four versions of the "native" *GADD45A-nLuc* system, creating both transcriptional and translational fusion constructs either with or without a degron tag (hPEST) (Fig. S7A). Luciferase levels were detectable in all four versions under basal conditions, and constructs lacking the degron tag were inducible by p53 (nutlin-3A) and ISR stimulating (tunicamycin) conditions (Fig. S3B), consistent with our results measuring native GADD45A mRNA expression (Fig. 6B). All subsequent experiments utilize the *GADD45A-nLuc* translational fusion lacking the degron tag due to the highest signal-to-noise ratio in our initial tests (Fig. S3B).

To confirm that the putative *cis*-element in the 3rd intron is essential for *GADD45A-nLuc* reporter activity, we characterized luciferase activity in response to mutation or deletion of nucleotides predicted to be critical for binding of p53 and/or ATF4. The intronic

enhancer has conserved p53RE and AP1 motifs that were previously reported to be required for ionizing radiation induced *GADD45A* expression (Chin et al., 1997; Daino et al., 2006; Smeenk et al., 2008). We additionally identified one canonical ATF4 motif (TGATGAAA, minus strand, Fig. 7C) using the JASPAR database. ATF/AP1 transcription family motifs are highly similar (Bejjani et al., 2019) (Fig. 7C, S4) and ATF4 can form heterodimers with other AP1 family members (Hai and Curran, 1991; Podust et al., 2001; Mann et al., 2013), thus we included mutants of both motifs to identify true ISR response element in the *GADD45A* enhancer. The wild-type *GADD45A-nLuc* reporter system responds to the p53 and ISR pathways similar to the native *GADD45A gene* (Fig. 7D). An intact p53RE motif was required for maximal enhancer-driven transcription under basal conditions and in agreement with previous work (Daino et al., 2006). Disrupting this motif (Fig. 7C) resulted in low expression levels similar to deletion of the entire 250bp DHS region suggesting that p53 is a major regulator of basal *GADD45A* transcription. Nutlin-3A-mediated transcriptional activation was completely dependent on the p53RE motif, whereas the ATF4 and AP1 motifs were dispensable for p53-mediated induction (Fig. 7D). Disrupting the predicted ATF4 motif had no effect on basal or tunicamycin-induced expression whereas disrupting the AP1 motif decreased basal activity and tunicamycin-mediated induction, suggesting that ISR pathway is regulated, at least partially, through the AP1 motif. Both the p53 and AP1 motifs appear to play key roles in the basal expression of *GADD45A,* but the motifs appear to be functionally distinct in response to p53 and ISR-stimulating conditions. We also included combinatorial motif mutants to investigate whether transcription factors binding to these motifs are activating independently. If the predicted ATF4 motif was not functional, one would expect that the double inactivation of p53RE and ATF4 motif would behave as p53RE mutant and would still be inducible by tunicamycin. In contrast, we observed lack of tunicamycin-mediated induction when the reporter had combined p53RE and ATF4 motif mutations. In fact, all constructs that included ATF4 and/or AP1 mutations in different combinations were not inducible by tunicamycin. It is possible that the ATF4 motif is not required under normal conditions but could act redundantly in the absence of the preferred AP1 motif.

Nucleotide-level characterization of the *GADD45A* enhancer reveals critical regulatory sequences

Enhancers are generally regulated by multiple transcription factors (TFs) working in a combinatorial fashion, with transcription factors acting positively or negatively depending on context (Kim and Wysocka, 2023). p53 binding primarily positively regulates enhancer activity, although the extent to which additional transcription factors are required for p53-dependent *trans*-activation remains an open question (Verfaillie et al., 2016; Catizone et al., 2020). Our observations suggest that the AP1 motif adjacent to the p53 response element in the *GADD45A* intronic enhancer is required for maximal transcriptional output mediated by the enhancer, but is not required for p53-dependent induction. Conversely, this AP-1 binding site is strictly required for tunicamycin-induced enhancer activity, suggesting that the regulatory potential of this enhancer is context-dependent. The *GADD45A* intron 3 enhancer is predicted to encode at least 10 distinct TF motifs (JASPAR 2022). To identify additional TF motifs regulating context-dependent enhancer activity, we measured basal and stimulus-dependent enhancer activity using STARRSeq (self-transcribing active regulatory region sequencing) (Muerdter et al., 2018). We performed nucleotide-resolution saturating mutagenesis with all possible substitutions or single nucleotide deletion at every position within the putative 250 bp intron 3 enhancer (Fig. 8A). First, this library was transiently transfected into the HCT116 wild-type and p53 null cell lines to assess p53 dependence. Cells were also treated with DMSO, nutlin-3A, or tunicamycin to measure p53 or ISR-mediated activation of the *GADD45A* enhancer reporter library (Fig. S4). Overall, the majority of single-nucleotide substitutions and deletions had little or no effect on basal or drug-induced activity (Fig. S4).

Consistent with our *GADD45A*- full gene reporter assays (Fig 7D), nucleotide substitutions and deletions at consensus motif positions with high predicted importance for p53 binding severely diminished enhancer activity in wild-type HCT116 cell line (Fig. 8C), with near perfect concordance to the canonical p53 RE motif. Changes in the critical half-site positions of p53RE (nucleotide positions 78-81 and 88-91) consistently disrupted enhancer-driven transcriptional activation. The majority of nucleotide substitutions in the 6 bp spacer between the half-sites had a minor to no effect on enhancer function (nucleotide positions 83-87). For example, T>A or T>C substitutions at the first position of the spacer are well-tolerated, but in agreement with known p53 binding preferences, T>G substitution reduced enhancer activity. T>C (position 3 of the spacer) and G>A (position 6) substitutions increased enhancer activity, again mirroring the shift closer to consensus p53 binding preferences. Conversely, all single nucleotide deletions disrupted enhancer activity, illustrating the well-studied importance of spacing between half-sites for p53 binding and activity (el-Deiry et al., 1992) (Fig. 8C).

Comparison of nucleotide substitutions between WT and p53 null conditions suggests the majority of the substitutions showing altered activity require an intact p53 response, with the exception of A85G and A86G substitutions. Although these nucleotide changes are predicted to be more similar to the consensus sequence than wild-type RE and display increased enhancer activity, they also show increased activity in p53 null cells, suggesting these substitutions may result in a *de novo* activating TF motif or disruption of a repressive TF element. Overall, loss-of-function substitutions in the p53RE did not display reduced enhancer activity in p53 null cells, as the genetic loss of p53 is expected to be epistatic with mutation of the p53RE (Fig. 8B). Nucleotide-resolution mutagenesis of the well-defined p53RE suggest that our STARRseq assay is suitable for high-throughput mutagenesis and identification of additional factors important for stress-dependent *GADD45A* enhancer.

We identified the AP1(FOS::JUN) site downstream of the p53RE, and not the predicted ATF4 upstream element, to be important for both basal- and tunicamycin-induced enhancer activity using traditional reporter gene assays (Fig. 7D). Disruption of the upstream ATF4 element in the saturating mutagenesis STARRseq assay had little to no effect on enhancer activity, whereas we observed a marked decrease in enhancer activity when the AP1 motif was disrupted in either WT or p53 null cell line (Fig. 8C, S4). The loss of activity in response to AP1 motif substitutions in p53 null lines further suggests combinatorial roles of these two elements in driving basal enhancer activity. Similar to our analysis with the p53RE, specific substitutions to the AP1 (FOS::JUN) motif demonstrates a clear dependence for known AP1 family binding preferences on enhancer activity. C>G/T substitutions at position 131 have increased activity, presumably representing a shift closer to the consensus AP1 motif. The most sensitive positions to nucleotide substitutions were the two palindromic half-sites ('TG' and 'CA') and nucleotide deletions predicted to disrupt spacing between those half-sites (Fig. 8C).

Our STARRSeq assay for the *GADD45A* intron 3 enhancer revealed multiple nucleotide substitutions with increased or decreased activity compared to the wild-type sequence. Individual nucleotide changes can disrupt TF motifs important for wild-type *GADD45A* enhancer activity, but could also represent varied activity due to *de novo* creation of TF binding sites or experimental noise. Therefore, to identify other true positive TF motifs, we focused our analysis on contiguous 6+ nucleotide regions that display altered activity when (1) multiple substitutions and deletions at the same position have similar effects, (2) changes in several adjacent positions have similar effect, and (3) motif mutations have negative effect on the expression and thus are potentially bound by activators. Using such criteria, we identified 3 other regions that may positively regulate *GADD45A* enhancer activity. Each of these regions overlap a specific predicted TF motif, ETV6, AP1/BACH1 or GLIS3/POU6F. AP1 members and BACH1 are part of the broader bZIP family of DNA binding proteins and have highly similar motif preferences. Consistent with the p53RE and the AP1 (FOS::JUN) sites, nucleotide substitutions at positions predicted to be important for either AP1 or BACH1 binding display reduced enhancer activity (Fig. 8C). These effects are observed in both WT and p53 null cell lines, suggesting this motif contributes to basal enhancer function in a p53-independent context. An A>C substitution at position 181 strongly increases enhancer activity, likely due to C adhering more closely to the predicted consensus binding motif for both AP1 and BACH1 dimers. Nucleotide deletions at any position had reduced enhancer activity, whereas we observed a position-specific effect of substitutions that mirror the consensus nucleotide preferences. Our saturating mutagenesis approach validates the critical role of the previously characterized p53 and AP1 binding sites in the positive regulation of the *GADD45A* enhancer, and revealed putative, novel TF motifs that may contribute to basal or induced enhancer activity.

Validation of the STARRseq-defined effects of nucleotide substitutions within the *GADD45A* enhancer via a native-context reporter assay activity.

To assess whether nucleotide substitutions in newly identified *GADD45A* enhancer motifs would have the same effect in a native gene context, we tested a series of 'upregulating' and 'downregulating' substitutions in our *GADD45A-nLuc* reporter system (Fig. 9). All *GADD45A-nLuc* enhancer mutants were transiently transfected into HCT116 wild-type and p53 null and treated with DMSO, nutlin-3A and tunicamycin. The AP1/BACH1(A181C) substitution moves this motif closer to the consensus sequence and is expected to improve binding and subsequent activation of *GADD45A*, whereas G177A would likely have the opposite effect. Indeed using the native reporter system demonstrates that these substitutions behave as predicted from the MPRA-based saturating mutagenesis approach (Fig. 8C, 9B). We next assessed how substitutions in the overlapping GLIS3 and POU6F2 motifs affect enhancer activity in the more native context. All of the nucleotide substitutions led to increased activity in the MPRA, suggesting these motifs and their bound factors may act to repress

GADD45A transcription. In the native reporter system, substitutions in this overlapping GLIS3/POU6F motif led to increased activity (Fig. 9B), further suggesting that this sequence restrains activity of the *GADD45A* enhancer.

Results from native reporter gene assays measuring the activity of nucleotide substitutions in the putative ETV6 motif located between the p53 and AP1 motifs were more nuanced. ETV6 is an ETS-family transcription factor and most frequently acts as a repressor (Lopez et al., 1999). The ETV6 A113G substitution, which led to consistently increased activity in the MPRA, displayed increased Nutlin-3A/p53-induced activity, but did not affect expression under basal or tunicamycin-treated conditions. The A112T substitution, predicted to reduce enhancer activity, actually displayed higher levels of nutlin-3A-induced activity in HCT116 WT p53 using the native reporter system. Interestingly, both the ETV6 A112T and A113G substitutions led to diminished enhancer activity across all treatment conditions in HCT116 p53 null. These data suggest a potential context-dependence of the ETV6 motif in regulation of *GADD45A* enhancer activity, with motif disruptions leading to varied effects depending on the presence of p53.

Discussion

In this study, we present a comparative analysis of the dynamic transcriptome landscape and unique and shared gene regulatory strategies between two fundamental cell stress responses. We demonstrate the p53 gene regulatory network and the ATF4-driven Integrated Stress Response pathway, although generally controlling distinct genes, converge on a set of common transcriptional targets related to metabolic control and apoptosis. Our study provides direct evidence that these common transcriptional targets require p53 during the DNA damage response, but not during activation of the ISR. Conversely, stress-dependent transcriptional activation of these target genes requires ATF4 during the ISR, with ATF4 being dispensable under p53-activating conditions. The genetic dependence of these transcriptional responses parallels the well-studied stress-evoked stabilization of p53 and translation of ATF4 (Kastan et al., 1991; Vattem and Wek, 2004), which is further supported by our observations that neither p53 nor ATF4 levels increase in response to activation of the other pathway (Fig. 1B, 2A, D). Importantly, these data are consistent with recent work suggesting that targeted activation of the ISR can activate specific p53 gene targets in p53-deficient cells and promote apoptosis(Hernandez Borrero et al., 2021; Tian et al., 2021). Similarly, chemical inhibition of the phosphatase PPM1D leads to increased ATF4 activity which synergized with p53 activation to amplify expression of some p53 target genes and increased cell death (Andrysik et al., 2022). These data now clearly point towards a potential therapeutic strategy broadly applicable across cancers regardless of *TP53* genetic status. Combined treatment with non-genotoxic activators of p53 (like MDM2 inhibitors) and chemical induction of the ISR pushes cells towards an apoptotic/cell death fate, which could overcome the reported limitations of MDM2 inhibition alone without direct genotoxic effects (Aziz et al., 2011). Numerous small molecules that restore p53 function in tumors with p53 missense mutations are in active development and their potential efficacy may be bolstered by combined ISR-mediated activation. These approaches are especially attractive given the non-genotoxic nature and the relatively large number of experimental compounds and approved drugs known to activate the p53 and ISR pathways.

Both the p53-dependent gene regulatory network and the ATF4-driven ISR are antiproliferative, either through induction of apoptosis or through direct or indirect control of the cell cycle. p53 canonically mediates its cell cycle control through *CDKN1A/*p21 and other members of the cell cycle control network, like *CCNG1* (Jensen, 2003). The p53 network appears to have built-in “redundancy” or “robustness”, whereby loss of one or more antiproliferative strategies, like cell cycle arrest, does not appreciably alter overall tumor suppressor function. These shared genes, then, may represent an additional layer of redundancy to tumor suppressor functions of p53 through metabolic control. At least four of the shared direct target genes of p53 and ATF4 (*DDIT4, GADD34, SESN2,* and *GDF15)* are antiproliferative via inhibition of mTOR signaling (Budanov and Karin, 2008; Gambardella et al., 2020; Lockhart et al., 2020; Aguilar-Recarte et al., 2021; Coronel et al., 2022). *ATF3* is also intimately involved in the coordination of cell cycle progression via control of serine, nucleotide, and glucose metabolism (Ku and Cheng, 2020; Di Marcantonio et al., 2021). It is tempting to speculate that these genes represent a “core” that is repurposed by numerous cell stress response pathways to enact an anti-proliferative strategy working through the central energy regulator mTOR. Thus, investigations into the regulation of these targets in response to stress conditions regulated by other master transcription factors such as hypoxia (HIF1α), heat shock (HSF1), inflammation (IRF/STAT), xenobiotics (AHR), and infection (NF-kB), may be warranted.

Taken together, our results and prior work demonstrate previously underappreciated crosstalk between the p53 and ISR transcriptional networks. Although each transcription factor is not required for the other to induce "common targets" or their pathway-specific genes, p53 does appear to indirectly regulate ATF4-dependent transcription in multiple ways. We observe a decrease in the total basal and ISR-mediated abundance of ATF4-specific targets in p53-deficient cells, including the well-defined ATF4-specific target *ASNS* (Fig. 1E). These observations may partially be explained by the reduction in ATF4 mRNA and protein levels seen in p53-deficient cells (Fig. 2A, D). We and others note a lack of p53 engagement with the *ATF4* locus and no change in *ATF4* transcription in response to p53 activation (Sammons et al., 2020; Andrysik et al., 2022), suggesting ATF4 indirect regulation by p53-dependent genes, but not direct p53 binding at *ATF4*. Reduced ATF4 protein expression may be a direct consequence of reduced mRNA abundance, but additional regulation at the translational control level is possible given p53's ability to broadly regulate protein synthesis (Loayza-Puch et al., 2013; Zaccara et al., 2014; Andrysik et al., 2017; Tameire et al., 2019).

We sought to further dissect this crosstalk between p53 and ATF4 by examining how their interaction DNA-encoded gene regulatory elements controls transcription of these common target genes. Our results examining the regulation of *ATF3* and *GADD45A* provide mechanistic detail into how these genes can be independently activated by both p53 and ATF4. Upon ISR induction, ATF4 binds to specific response element sequences within the *ATF3* promoter. The ability of ATF4 to activate ATF3 transcription does not depend on p53 or on a distal enhancer element bound by p53, as shown in both knockout and CRISPRi experiments. Similarly, p53 activates ATF3 expression via this distal enhancer after knockdown of ATF4 via shRNA. Thus, p53 and ATF4 mediate stress-dependent *ATF3* expression independently through spatially distinct regulatory elements.

Stress-dependent *GADD45A* expression, in contrast, is controlled by a single regulatory element bound by both p53 and ATF4. STARRSeq-based saturating mutagenesis of this *GADD45A* enhancer provided nucleotide-level resolution of DNA elements that control enhancer activity. Consistent with our genetic, biochemical, and reporter gene analyses, this assay demonstrated that the putative binding motifs for p53 and ATF4 had the most significant impact on enhancer activity and *GADD45A* expression. Nucleotide substitutions at positions predicted to be critical for binding affinity and specificity had the most profound effect on enhancer function. This is true for predicted loss-of-function nucleotide substitutions, but also substitutions that are predicted to improve transcription factor binding by moving the motif closer to the consensus. These data suggest that MPRA-style assays like STARRseq are suitable for examining the impact of sequence differences in p53-bound elements resulting from natural or disease-associated human variation (Fig. S4). This impact has not been comprehensively explored, but certain gain-of-function variants with pro-tumorigenic activity have been reported (Menendez et al., 2007; Zeron-Medina et al., 2013). We also identified and validated three additional transcription factor binding motifs that directly impact enhancer activity. Sequence-based motif prediction methods identify numerous putative transcription factor binding sites within the *GADD45A* enhancer that did not alter enhancer activity in this context. Enhancers have well-defined cell lineage-dependent activity based on the specific combination of transcription factors that may be present (Zeitlinger, 2020; Kim et al., 2021), thus, we cannot rule out that these predicted motifs may be functional in other settings. Thus, a combination of unbiased saturating mutagenesis screening across diverse cell types and sequence-based motif analyses may help to refine and improve the ability to predict functional elements within regulatory elements.

Our results examining p53 and ATF4-mediated induction of *GADD45A* provide new insight into the complex interplay between multiple transcription factors at stress-dependent enhancers. The p53RE was absolutely critical for nutlin-3A-induced expression of *GADD45A,* whereas all other motifs were dispensable, including the AP1 site critical for ATF4-mediated expression. These new functional motifs, along with the p53RE, are also unnecessary for ATF4-dependent induction. These observations mirror prior studies demonstrating that p53-induced enhancer activity solely depends on p53 binding and that p53 motifs are the strongest predictor of high enhancer activity (Verfaillie et al., 2016; Younger and Rinn, 2017). While a global analysis of ATF4-dependent regulatory elements using MPRA-style approaches has not been reported, our results suggest that like p53, ATF4 may not require other transcription factors to induce stress-dependent enhancer activity. This is an attractive model for stress-dependent transcription factors, as their gene regulatory activity would remain robust even in the absence of other factors. Recent work, though, suggests that p53-dependent enhancer activity relies on other transcription factors in different contexts, primarily through cell lineage-dependent regulation of chromatin structure. An important caveat

to MPRA and reporter gene studies is the lack of chromatin context that might mask the requirement for other transcription factors, especially those that might alter chromatin accessibility. Although additional work is needed to further explore context-dependent transcription factor requirements, our results provide additional support for autonomous activity of p53 and ATF4 during stress-dependent enhancer activation.

Although they appear unnecessary for stress-mediated induction, the newly identified transcription factor motifs (ETV6, AP1:BACH1, GLIS3/POU6F) modulate *GADD45A* enhancer activity in unstressed conditions. This suggests these sites are bound by transcription factors and also suggests a context in which additional transcription factors may regulate p53- or ATF4-bound enhancers. The absence of these additional motifs, and presumably the factors that bind them, affects the overall expression level of *GADD45A*. Thus, while p53 and ATF4 can still evoke additional enhancer activity, absence of these motifs leads to altered total levels of *GADD45A* expression. Similarly, mutation of the ATF4 binding site reduces *GADD45A* transcription in unstressed conditions but permits p53-mediated activation albeit at a lower total mRNA output. These observations suggest that *GADD45A* levels are ultimately controlled by a combination of all functional transcription factor motifs, consistent with the billboard or additive model for enhancer function and suggest that differential enhancer "grammar" is needed for basal versus stress-dependent transcriptional regulation.

Acknowledgments

The authors would like to thank the University at Albany Center for Functional Genomics for sequencing and analytical support. SAD was supported by a University at Albany RNA Institute Fellowship. This work was supported by NIH NIGMS R35 GM138120.

Figure Legends

Figure 1. ATF3 is a p53 target gene that is activated via the Integrated Stress Response (ISR) in a p53-independent manner.
Western Blot analysis of A) ATF3 and B) p53 with GAPDH as a loading control in HCT116 p53 WT (left) and p53 null cells (right) following a 6h treatment with DMSO, 5 μM Nutlin-3A (NUT), 100 μM etoposide (ETOP), 2 μM Tunicamycin (TM) or 2mM Histidinol (HisOH). Gene expression analysis of the C) *ATF3* gene D) *CDKN1A* gene and E) *ASNS* gene in HCT116 p53 WT (black) and HCT116 p53 null (pink) cells in response to 6h treatment with aforementioned stimuli. All statistical comparisons were computed using a one-way ANOVA test. *p<0.05, **p<0.01, ***p<0.001, ****p<0.0001.

Figure 2. ATF4 and p53 independently regulate expression of *ATF3*.
Western Blot analysis of ATF4 with GAPDH as a loading control in A) HCT116 p53 WT (left) and p53 null cells (right), B) HCT1116 p53 WT (left) and p53 null cells (right) containing shRNA constructs targeting *ATF4* (ATF4 shRNA) or a non-targeting control (Scramble shRNA) and C) HAP1 parental and ATF4 null (ATF4KO) cells. Gene expression analysis of the *ATF4* gene in D) HCT116 cells, E) HCT116 *ATF4* knockdown (ATF4KD) cells and F) HAP1 cells. Gene expression analysis of *ATF3* in G) HCT116 ATF4 knockdown cells and H) HAP1 ATF4KO cells. Gene expression analysis of *ASNS* in I) HCT116 ATF4KD cells and J) HAP1 ATF4KO cells. Cells were harvested for each experiment 6h post-treatment with DMSO, 10 μM nutlin-3A (NUT), 100 μM etoposide (ETOP), 2 μM tunicamycin (TM) or 2 mM histidinol (HisOH). All statistical comparisons were computed using a one-way ANOVA test. *p<0.05, **p<0.01, ***p<0.001, ****p<0.0001.

Figure 3. ATF4 and p53 occupy distinct regulatory regions in the *ATF3* gene locus.
A) Known motif enrichment analysis of the high-confidence peak set reveals the predicted ATF4 motif as the most highly-enriched motif within this dataset. B) *de novo* motif analysis of high-confidence peak set shows enrichment of ATF4 motif. C) Enrichment of CUT&RUN sequencing tags after 6h drug treatments as indicated. D) Genome browser view of the *ATF3* gene locus displaying ATF4 CUT&RUN data (black) and p53 ChIP-Seq data (green) following 6 hr treatment with various stress stimuli: DMSO (vehicle control), 5 μM nutlin-3A (NUTLIN), 100 μM etoposide (ETOP), 2 μM tunicamycin (TM), or 2mM histidinol (HisOH) from -1000bp and +1000bp from peak center.

Figure S1.
A) Intersection of ATF4 CUT&RUN peaks for the three biological replicates of HCT116 p53 WT cells treated with 2 μM tunicamycin for 6h. B) Intersection of ATF4 CUT&RUN peaks for the three biological replicates of HCT116 p53 WT cells treated with 2mM histidinol for 6 hrs. C) A set of high-confidence ISR-activated ATF4 binding events created by considering only peaks called out from 5 out of the 6 experiments with ISR-activating treatments: 2 μM tuncamycin and 2 mM histidinol. D) Genome browser view of the *ASNS* gene locus displaying ATF4 CUT&RUN data (black) and p53 ChIP-Seq data (green) in HCT116 p53 WT cells following 6 hr treatment with various stress stimuli, including: DMSO (vehicle control), 5 μM nutlin-3A

(NUTLIN), 100 μM etoposide (ETOP), 2 μM Tuncamycin (TM), and 2mM histidinol (HisOH).

Figure 4. *ATF3* induction by the ISR does not require the upstream enhancer element bound by p53.
A) Normalized luciferase values driven by the upstream *ATF3* DNase Hypersensitivity sites (DHS): ATF4-bound DHS, p53-bound DHS, p53bs Mutant, and the minimal promoter (negative control), in response to 16h treatment with DMSO, 5 μM nutlin-3A (NUT) or 2 μM tunicamycin (Tm) in HCT116 p53 WT and p53 null cells. B) Normalized luciferase values driven by the (-107/+35) *ATF3* promoter sequence (WT *ATF3* promoter) and constructs containing mutations in specific ATF4 response elements: CARE, CRE, CARE/CRE, in response to 16 h treatment with DMSO, 2 μM tunicamycin (Tm), or 2mM histidinol (HisOH) in HAP1 parental and ATF4KO cells. C) Genome browser view of the *ATF3* gene locus displaying the location of dCas9-KRAB gRNA targets and the genomic coordinates spanning these targets relevant to panel D. D) RT-qPCR analysis of the *ATF3* gene in response to 6 h treatment with DMSO, 100 μM etoposide (ETOP) or 2 μM Tunicamycin (TM) in HCT116 p53 WT cells where dCas9-KRAB is targeting regions at off-target control enhancer (blue), intergenic control (orange and green), the p53-bound *ATF3* enhancer element (purple) or *ATF3* promoter (red) for transcriptional repression. RT-qPCR analysis of the C) *ASNS* gene, and D) *CDKN1A*/*p21* gene, following a 6h treatment with various stress stimuli. Statistical comparisons for nascent expression levels were computed using a one-way ANOVA test. Statistical comparisons for fold change induction levels were compute using an unpaired t-test. *p<0.05, **p<0.01, ***p<0.001, ****p<0.0001.

Figure 5. Global transcriptome analysis identifies common gene regulatory targets of the p53 GRN and the ISR
A) Intersection of genes upregulated in HCT116 p53 WT cells treated with 5 μM nutlin-3A, 100 μM etoposide, 2mMTunicamycin, and 2 μM histidinol, when compared to vehicle control (DMSO) for 6h. B) Heatmap displaying fold change values for the 27 common targets identified in panel A. C) Table displaying the gene symbols for the 27 common target Ensembl gene IDs identified in panel A. Gene ontology analysis of the genes commonly D) upregulated and E) downregulated, in response to these various stress stimuli.

Figure S2.
RNASeq analysis of differential gene expression in HCT116 WT and p53 null cell lines in response to various stimuli, including 5 μM nutlin-3A (A, E), 100 μM etoposide (B, F), 2 μM tunicamycin (C, G), or 2mM histidinol (D, H), compared to vehicle control (DMSO). Gene ontology analysis of the genes upregulated (A-D) and downregulated (E-H) in response to treatments. (i-L) Enhanced volcano plots displaying differential gene expression in HCT116 WT cells treated stimuli as described above.

Figure 6. Parallel stress-dependent networks converge at activation of a common set of target genes.
RT-qPCR analysis of the *ATF3, GADD45a*, *SESN2,* and *GDF15* gene in A-D) HCT116 p53 WT and p53 null cells, E-H) MCF10A p53 WT and p53 null cells, and I-L) HAP1 parental and ATF4KO cells, following a 6h treatment with DMSO, 100 μM etoposide (ETOP), or 2 μM Tunicamycin (Tm). All statistical comparisons were computed using a one-way ANOVA test. *p<0.05, **p<0.01, ***p<0.001, ****p<0.0001.

Figure S3. Comparison of *GADD45A-nLuc* reporter expression in the presence or absence of T2A skipping peptide and/or hPEST degradation tag.
(A) Schematic representation of various *GADD45A-nLuc* reporter constructs with T2A or hPEST included in the 3' end. (B) Normalized luciferase expression values from *GADD45A-nLuc* reporters transfected into HCT116 WT cell line and 16h treatment with DMSO, nutlin-3A and tunicamycin as indicated in the legend. Presence ('+') or absence (grey) of T2A or hPEST tags are indicated in the table below.

Figure 7. *GADD45A* as a reporter system to study DDR and ISR-dependent enhancers.
(A) Genome browser view with *GADD45A* locus displaying ATF4 CUT&RUN and p53 ChIP-Seq data (Andrysik et al., 2017) in HCT116 WT cell line following 6h treatment with DMSO, 2 mM histidinol (HisOH), 2 μM Tunicamycin (TM), and 5 μM nutlin-3A (NUT). Putative p53RE and ATF4 motif, GADD45A intron 3 enhancer location are indicated on the bottom, DNaseI hypersensitive sites (DHS) are marked in grey/black. (B) Schematic representation of the *GADD45A-nLuc* reporter construct with relevant enhancer sequence motifs highlighted in (C). (D) Normalized luciferase expression values using *GADD45A-nLuc* reporter transfected into HCT116 wt cell line and 16h treatment with DMSO, nutlin-3A and tunicamycin as indicated in the legend. Reporter constructs included wild-type, a negative control with 250 bp enhancer deletion ('No Enhancer') and various ATF4, AP1 and p53RE motif mutations alone or in combination as indicated in the table below ('wt' or 'mutant' in grey). Specific mutations in motifs are indicated in (C). Statistical comparisons

were generated using paired t-test: * p<0.05, ** p<0.01, *** p< 0.001, **** p<0.0001.

Figure 8. Nucleotide resolution of *GADD45A* enhancer sequence critical for promoter activation function. (A) Schematic illustrating *GADD45A* 250 nt enhancer mutagenesis screen using the STARRSeq system (hSTARRSeq_ORI). Substitutions and deletions of every nucleotide position are depicted as 'X'; p53RE in blue; open reading frame as 'ORF'; polyadenylation site as 'polyA'. (B) Heatmap representing expression mediated by each enhancer variant relative to the wild-type enhancer from the same cell line and treatment condition. Relative position in the enhancer (1-250 nt) is indicated on the *x*-axis. Each deletion ('Del') or base substitution ('A', 'C', 'G', 'T') is indicated as a row label. 'Grey' color in row 'Del' indicates a redundant position when >1 consecutive base is identical. Relevant motifs discussed in the text are highlighted (red dashed line) including: *GADD45A* native motif sequence, relative position, name ('p53RE', 'AP1') and PWM logos (JASPAR 2022) are in (C). Cell lines and treatment conditions are indicated above each heatmap.

Figure S4. Nucleotide resolution of *GADD45A* enhancer sequence critical for promoter activation function (extended). Heatmap representing expression mediated by each enhancer variant relative to the wild-type enhancer from the same cell line and treatment condition. Relative position in the enhancer (1-250 nt) is indicated on the *x*-axis. Each deletion ('Del') or base substitution ('A', 'C', 'G', 'T') is indicated as a row label. 'Grey' color in row 'Del' indicates a redundant position when >1 consecutive base is identical. Relevant motifs discussed in the text are highlighted (red dashed line) including: *GADD45A* native motif sequence, relative position, name ('ATF4', 'p53RE', 'AP1', 'GLIS3/POU6F') and PWM logos (JASPAR 2022). Cell lines and treatment conditions are indicated above each heatmap. (Top Row) Barplot highlighting SNPs found in *GADD45A* enhancer region from db155SNP database with expression values from HCT116 WT, DMSO experiment.

Figure 9. Other STARRSeq-identified motifs contribute only to basal *GADD45A* enhancer activity. (A) Schematic representation of the *GADD45A-nLuc* reporter construct with relevant enhancer sequence motifs highlighted in (B). (C) Normalized luciferase expression values using *GADD45A-nLuc* reporter transfected into HCT116 wild-type cell line and 16h treatment with DMSO, nutlin-3A and tunicamycin as indicated in the legend. Reporter constructs included wild-type construct, 250 bp enhancer deletion ('No Enhancer') as a negative control and various predicted transcription factor motif mutations as indicated on the *x*-axis. Specific mutations in transcription factor motifs based on the STARRSeq screen are indicated in (B). Statistical comparisons were generated using paired t-tests: * p<0.05, ** p<0.01, *** p< 0.001, **** p<0.0001.

Table S1. List of plasmids and oligonucleotides used in this study.

References

Advani, V. M., and Ivanov, P. (2019). Translational Control under Stress: Reshaping the Translatome. *BioEssays* 41, 1900009. doi: 10.1002/bies.201900009.

Aguilar-Recarte, D., Barroso, E., Gumà, A., Pizarro-Delgado, J., Peña, L., Ruart, M., et al. (2021). GDF15 mediates the metabolic effects of PPARβ/δ by activating AMPK. *Cell Rep.* 36, 109501. doi: 10.1016/j.celrep.2021.109501.

Andreeff, M., Kelly, K. R., Yee, K., Assouline, S., Strair, R., Popplewell, L., et al. (2016). Results of the Phase I Trial of RG7112, a Small-Molecule MDM2 Antagonist in Leukemia. *Clin. Cancer Res.* 22, 868–876. doi: 10.1158/1078-0432.CCR-15-0481.

Andrysik, Z., Galbraith, M. D., Guarnieri, A. L., Zaccara, S., Sullivan, K. D., Pandey, A., et al. (2017). Identification of a core TP53 transcriptional program with highly distributed tumor suppressive activity. *Genome Res.* 27, 1645–1657. doi: 10.1101/gr.220533.117.

Andrysik, Z., Sullivan, K. D., Kieft, J. S., and Espinosa, J. M. (2022). PPM1D suppresses p53-dependent transactivation and cell death by inhibiting the Integrated Stress Response. *Nat. Commun.* 13, 7400. doi: 10.1038/s41467-022-35089-5.

Aziz, M. H., Shen, H., and Maki, C. G. (2011). Acquisition of p53 mutations in response to the non-genotoxic p53 activator Nutlin-3. *Oncogene* 30, 4678–4686. doi: 10.1038/onc.2011.185.

Bejjani, F., Evanno, E., Zibara, K., Piechaczyk, M., and Jariel-Encontre, I. (2019). The AP-1 transcriptional complex: Local switch or remote command? *Biochim. Biophys. Acta BBA - Rev. Cancer* 1872, 11–23. doi: 10.1016/j.bbcan.2019.04.003.

Bray, N. L., Pimentel, H., Melsted, P., and Pachter, L. (2016). Near-optimal probabilistic RNA-seq quantification. *Nat. Biotechnol.* 34, 525–527. doi: 10.1038/nbt.3519.

Budanov, A. V., and Karin, M. (2008). p53 Target Genes Sestrin1 and Sestrin2 Connect Genotoxic Stress and mTOR Signaling. *Cell* 134, 451–460. doi: 10.1016/j.cell.2008.06.028.

Bushnell, B., Rood, J., and Singer, E. (2017). BBMerge – Accurate paired shotgun read merging via overlap. *PLOS ONE* 12, e0185056. doi: 10.1371/journal.pone.0185056.

Bykov, V. J. N., Eriksson, S. E., Bianchi, J., and Wiman, K. G. (2018). Targeting mutant p53 for efficient cancer therapy. *Nat. Rev. Cancer* 18, 89–102. doi: 10.1038/nrc.2017.109.

Catizone, A. N., Uzunbas, G. K., Celadova, P., Kuang, S., Bose, D., and Sammons, M. A. (2020). Locally acting transcription factors regulate p53-dependent cis-regulatory element activity. *Nucleic Acids Res.* 48, 4195–4213. doi: 10.1093/nar/gkaa147.

Chaudhari, H. G., and Cohen, B. A. (2018). Local sequence features that influence AP-1 cis-regulatory activity. *Genome Res.* 28, 171–181. doi: 10.1101/gr.226530.117.

Chavel, C. A., Dionne, H. M., Birkaya, B., Joshi, J., and Cullen, P. J. (2010). Multiple Signals Converge on a Differentiation MAPK Pathway. *PLoS Genet.* 6, e1000883. doi: 10.1371/journal.pgen.1000883.

Chen, B. P., Wolfgang, C. D., and Hai, T. (1996). Analysis of ATF3, a transcription factor induced by physiological stresses and modulated by gadd153/Chop10. *Mol. Cell. Biol.* 16, 1157–1168. doi: 10.1128/MCB.16.3.1157.

Chen, E. Y., Tan, C. M., Kou, Y., Duan, Q., Wang, Z., Meirelles, G. V., et al. (2013). Enrichr: interactive and collaborative HTML5 gene list enrichment analysis tool. *BMC Bioinformatics* 14, 128. doi: 10.1186/1471-2105-14-128.

Chen, H., Pan, Y.-X., Dudenhausen, E. E., and Kilberg, M. S. (2004). Amino Acid Deprivation Induces the Transcription Rate of the Human Asparagine Synthetase Gene through a Timed Program of Expression and Promoter Binding of Nutrient-responsive Basic Region/Leucine Zipper Transcription Factors as Well as Localized Histone Acetylation. *J. Biol. Chem.* 279, 50829–50839. doi: 10.1074/jbc.M409173200.

Chin, P. L., Momand, J., and Pfeifer, G. P. (1997). In vivo evidence for binding of p53 to consensus binding sites in the p21 and GADD45 genes in response to ionizing radiation. *Oncogene* 15, 87–99. doi: 10.1038/sj.onc.1201161.

Choi, J., Lysakovskaia, K., Stik, G., Demel, C., Söding, J., Tian, T. V., et al. (2021). Evidence for additive and synergistic action of mammalian enhancers during cell fate determination. *eLife* 10, e65381. doi: 10.7554/eLife.65381.

Chowdhury, P., Lin, G. E., Liu, K., Song, Y., Lin, F.-T., and Lin, W.-C. (2014). Targeting TopBP1 at a convergent point of multiple oncogenic pathways for cancer therapy. *Nat. Commun.* 5, 5476. doi: 10.1038/ncomms6476.

Coronel, L., Häckes, D., Schwab, K., Riege, K., Hoffmann, S., and Fischer, M. (2022). p53-mediated AKT and mTOR inhibition requires RFX7 and DDIT4 and depends on nutrient abundance. *Oncogene* 41, 1063–1069. doi: 10.1038/s41388-021-02147-z.

Daino, K., Ichimura, S., and Nenoi, M. (2006). Both the basal transcriptional activity of the GADD45A gene and its enhancement after ionizing irradiation are mediated by AP-1 element. *Biochim. Biophys. Acta BBA - Gene Struct. Expr.* 1759, 458–469. doi: 10.1016/j.bbaexp.2006.09.005.

Di Marcantonio, D., Martinez, E., Kanefsky, J. S., Huhn, J. M., Gabbasov, R., Gupta, A., et al. (2021). ATF3 coordinates serine and nucleotide metabolism to drive cell cycle progression in acute myeloid leukemia. *Mol. Cell* 81, 2752-2764.e6. doi: 10.1016/j.molcel.2021.05.008.

Ding, W.-X., Ni, H.-M., Gao, W., Hou, Y.-F., Melan, M. A., Chen, X., et al. (2007). Differential Effects of Endoplasmic Reticulum Stress-induced Autophagy on Cell Survival*. *J. Biol. Chem.* 282, 4702–4710. doi: 10.1074/jbc.M609267200.

Ebert, S. M., Al-Zougbi, A., Bodine, S. C., and Adams, C. M. (2019). Skeletal Muscle Atrophy: Discovery of Mechanisms and Potential Therapies. *Physiology* 34, 232–239. doi: 10.1152/physiol.00003.2019.

el-Deiry, W. S., Kern, S. E., Pietenpol, J. A., Kinzler, K. W., and Vogelstein, B. (1992). Definition of a consensus binding site for p53. *Nat. Genet.* 1, 45–49. doi: 10.1038/ng0492-45.

el-Deiry, W. S., Tokino, T., Velculescu, V. E., Levy, D. B., Parsons, R., Trent, J. M., et al. (1993). WAF1, a potential mediator of p53 tumor suppression. *Cell* 75, 817–825. doi: 10.1016/0092-8674(93)90500-p.

Fu, L., and Kilberg, M. S. (2013). Elevated cJUN expression and an ATF/CRE site within the ATF3 promoter contribute to activation of ATF3 transcription by the amino acid response. *Physiol. Genomics* 45, 127–137. doi: 10.1152/physiolgenomics.00160.2012.

Gambardella, G., Staiano, L., Moretti, M. N., De Cegli, R., Fagnocchi, L., Di Tullio, G., et al. (2020). GADD34 is a modulator of autophagy during starvation. *Sci. Adv.* 6, eabb0205. doi: 10.1126/sciadv.abb0205.

Garaeva, A. A., Kovaleva, I. E., Chumakov, P. M., and Evstafieva, A. G. (2016). Mitochondrial dysfunction induces *SESN* 2 gene expression through Activating Transcription Factor 4. *Cell Cycle* 15, 64–71. doi: 10.1080/15384101.2015.1120929.

Gilbert, L. A., Larson, M. H., Morsut, L., Liu, Z., Brar, G. A., Torres, S. E., et al. (2013). CRISPR-Mediated Modular RNA-Guided Regulation of Transcription in Eukaryotes. *Cell* 154, 442–451. doi: 10.1016/j.cell.2013.06.044.

Hai, T. (2006). "The ATF Transcription Factors in Cellular Adaptive Responses," in *Gene Expression and Regulation*, ed. J. Ma (New York, NY: Springer New York), 329–340. doi: 10.1007/978-0-387-40049-5_20.

Hai, T., and Curran, T. (1991). Cross-family dimerization of transcription factors Fos/Jun and ATF/CREB alters DNA binding specificity. *Proc. Natl. Acad. Sci.* 88, 3720–3724. doi: 10.1073/pnas.88.9.3720.

Hai, T., Wolfgang, C. D., Marsee, D. K., Allen, A. E., and Sivaprasad, U. (1999). ATF3 and stress responses. *Gene Expr.* 7, 321–335.

Hai, T., Wolford, C. C., and Chang, Y.-S. (2010). ATF3, a hub of the cellular adaptive-response network, in the pathogenesis of diseases: is modulation of inflammation a unifying component? *Gene Expr.* 15, 1–11. doi: 10.3727/105221610x12819686555015.

Han, J., Back, S. H., Hur, J., Lin, Y.-H., Gildersleeve, R., Shan, J., et al. (2013). ER-stress-induced transcriptional regulation increases protein synthesis leading to cell death. *Nat. Cell Biol.* 15, 481–490. doi: 10.1038/ncb2738.

Hashimoto, Y., Zhang, C., Kawauchi, J., Imoto, I., Adachi, M. T., Inazawa, J., et al. (2002). An alternatively spliced isoform of transcriptional repressor ATF3 and its induction by stress stimuli. *Nucleic Acids Res.* 30, 2398–2406. doi: 10.1093/nar/30.11.2398.

Hernandez Borrero, L., Dicker, D. T., Santiago, J., Sanders, J., Tian, X., Ahsan, N., et al. (2021). A subset of CB002 xanthine analogs bypass p53-signaling to restore a p53 transcriptome and target an S-phase cell cycle checkpoint in tumors with mutated-p53. *eLife* 10, e70429. doi: 10.7554/eLife.70429.

Jensen, M. (2003). Reduced hepatic tumor incidence in cyclin G1-deficient mice. *Hepatology* 37, 862–870. doi: 10.1053/jhep.2003.50137.

Jiang, H.-Y., Wek, S. A., McGrath, B. C., Lu, D., Hai, T., Harding, H. P., et al. (2004). Activating transcription factor 3 is integral to the eukaryotic initiation factor 2 kinase stress response. *Mol. Cell. Biol.* 24, 1365–1377. doi: 10.1128/MCB.24.3.1365-1377.2004.

Kastan, M. B., Onyekwere, O., Sidransky, D., Vogelstein, B., and Craig, R. W. (1991). Participation of p53 protein in the cellular response to DNA damage. *Cancer Res.* 51, 6304–6311.

Kilberg, M. S., Shan, J., and Su, N. (2009). ATF4-dependent transcription mediates signaling of amino acid limitation. *Trends Endocrinol. Metab.* 20, 436–443. doi: 10.1016/j.tem.2009.05.008.

Kim, D., Paggi, J. M., Park, C., Bennett, C., and Salzberg, S. L. (2019). Graph-based genome alignment and genotyping with HISAT2 and HISAT-genotype. *Nat. Biotechnol.* 37, 907–915. doi: 10.1038/s41587-019-0201-4.

Kim, D. S., Risca, V. I., Reynolds, D. L., Chappell, J., Rubin, A. J., Jung, N., et al. (2021). The dynamic, combinatorial cis-regulatory lexicon of epidermal differentiation. *Nat. Genet.* 53,

1564–1576. doi: 10.1038/s41588-021-00947-3.

Kim, S., and Wysocka, J. (2023). Deciphering the multi-scale, quantitative cis-regulatory code. *Mol. Cell* 83, 373–392. doi: 10.1016/j.molcel.2022.12.032.

Kocik, J., Machula, M., Wisniewska, A., Surmiak, E., Holak, T. A., and Skalniak, L. (2019). Helping the Released Guardian: Drug Combinations for Supporting the Anticancer Activity of HDM2 (MDM2) Antagonists. *Cancers* 11, 1014. doi: 10.3390/cancers11071014.

Ku, H.-C., and Cheng, C.-F. (2020). Master Regulator Activating Transcription Factor 3 (ATF3) in Metabolic Homeostasis and Cancer. *Front. Endocrinol.* 11, 556. doi: 10.3389/fendo.2020.00556.

Kuleshov, M. V., Jones, M. R., Rouillard, A. D., Fernandez, N. F., Duan, Q., Wang, Z., et al. (2016). Enrichr: a comprehensive gene set enrichment analysis web server 2016 update. *Nucleic Acids Res.* 44, W90–W97. doi: 10.1093/nar/gkw377.

Li, A., Zhao, F., Zhao, Y., Liu, H., and Wang, Z. (2021). ATF4-mediated GDF15 suppresses LPS-induced inflammation and MUC5AC in human nasal epithelial cells through the PI3K/Akt pathway. *Life Sci.* 275, 119356. doi: 10.1016/j.lfs.2021.119356.

Loayza-Puch, F., Drost, J., Rooijers, K., Lopes, R., Elkon, R., and Agami, R. (2013). p53 induces transcriptional and translational programs to suppress cell proliferation and growth. *Genome Biol.* 14, R32. doi: 10.1186/gb-2013-14-4-r32.

Lockhart, S. M., Saudek, V., and O'Rahilly, S. (2020). GDF15: A Hormone Conveying Somatic Distress to the Brain. *Endocr. Rev.* 41, bnaa007. doi: 10.1210/endrev/bnaa007.

Lopez, R. G., Carron, C., Oury, C., Gardellin, P., Bernard, O., and Ghysdael, J. (1999). TEL Is a Sequence-specific Transcriptional Repressor *. *J. Biol. Chem.* 274, 30132–30138. doi: 10.1074/jbc.274.42.30132.

Love, M. I., Huber, W., and Anders, S. (2014). Moderated estimation of fold change and dispersion for RNA-seq data with DESeq2. *Genome Biol.* 15, 550. doi: 10.1186/s13059-014-0550-8.

Lu, D., Wolfgang, C. D., and Hai, T. (2006). Activating transcription factor 3, a stress-inducible gene, suppresses Ras-stimulated tumorigenesis. *J. Biol. Chem.* 281, 10473–10481. doi: 10.1074/jbc.M509278200.

Mann, I. K., Chatterjee, R., Zhao, J., He, X., Weirauch, M. T., Hughes, T. R., et al. (2013). CG methylated microarrays identify a novel methylated sequence bound by the CEBPB|ATF4 heterodimer that is active in vivo. *Genome Res.* 23, 988–997. doi: 10.1101/gr.146654.112.

Mantovani, F., Collavin, L., and Del Sal, G. (2019). Mutant p53 as a guardian of the cancer cell. *Cell Death Differ.* 26, 199–212. doi: 10.1038/s41418-018-0246-9.

Margolin, J. F., Friedman, J. R., Meyer, W. K., Vissing, H., Thiesen, H. J., and Rauscher, F. J. (1994). Krüppel-associated boxes are potent transcriptional repression domains. *Proc. Natl. Acad. Sci. U. S. A.* 91, 4509–4513. doi: 10.1073/pnas.91.10.4509.

Menendez, D., Inga, A., Snipe, J., Krysiak, O., Schönfelder, G., and Resnick, M. A. (2007). A single-nucleotide polymorphism in a half-binding site creates p53 and estrogen receptor control of vascular endothelial growth factor receptor 1. *Mol. Cell. Biol.* 27, 2590–2600. doi: 10.1128/MCB.01742-06.

Moder, M., Velimezi, G., Owusu, M., Mazouzi, A., Wiedner, M., Ferreira da Silva, J., et al. (2017). Parallel genome-wide screens identify synthetic viable interactions between the BLM helicase complex and Fanconi anemia. *Nat. Commun.* 8, 1238. doi: 10.1038/s41467-017-01439-x.

Montesinos, P., Beckermann, B. M., Catalani, O., Esteve, J., Gamel, K., Konopleva, M. Y., et al. (2020). MIRROS: a randomized, placebo-controlled, Phase III trial of cytarabine ± idasanutlin in relapsed or refractory acute myeloid leukemia. *Future Oncol. Lond. Engl.* 16, 807–815. doi: 10.2217/fon-2020-0044.

Muerdter, F., Boryń, Ł. M., Woodfin, A. R., Neumayr, C., Rath, M., Zabidi, M. A., et al. (2018). Resolving systematic errors in widely used enhancer activity assays in human cells. *Nat. Methods* 15, 141–149. doi: 10.1038/nmeth.4534.

Neumayr, C., Pagani, M., Stark, A., and Arnold, C. D. (2019). STARR-seq and UMI-STARR-seq: Assessing Enhancer Activities for Genome-Wide-, High-, and Low-Complexity Candidate Libraries. *Curr. Protoc. Mol. Biol.* 128, e105. doi: 10.1002/cpmb.105.

Osada, M., Park, H. L., Park, M. J., Liu, J.-W., Wu, G., Trink, B., et al. (2007). A p53-type response element in the GDF15 promoter confers high specificity for p53 activation. *Biochem. Biophys. Res. Commun.* 354, 913–918. doi: 10.1016/j.bbrc.2007.01.089.

Pan, Y.-X., Chen, H., Thiaville, M. M., and Kilberg, M. S. (2007). Activation of the ATF3 gene through a co-ordinated amino acid-sensing response programme that controls transcriptional regulation of responsive genes following amino acid limitation. *Biochem. J.* 401, 299–307. doi: 10.1042/BJ20061261.

Podust, L. M., Krezel, A. M., and Kim, Y. (2001). Crystal Structure of the CCAAT Box/Enhancer-binding Protein β Activating Transcription Factor-4 Basic Leucine Zipper Heterodimer in the Absence of DNA *. *J. Biol. Chem.* 276, 505–513. doi: 10.1074/jbc.M005594200.

Qi, L. S., Larson, M. H., Gilbert, L. A., Doudna, J. A., Weissman, J. S., Arkin, A. P., et al. (2013). Repurposing CRISPR as an RNA-guided platform for sequence-specific control of gene expression. *Cell* 152, 1173–1183. doi: 10.1016/j.cell.2013.02.022.

Ramírez, F., Ryan, D. P., Grüning, B., Bhardwaj, V., Kilpert, F., Richter, A. S., et al. (2016). deepTools2: a next generation web server for deep-sequencing data analysis. *Nucleic Acids Res.* 44, W160–W165. doi: 10.1093/nar/gkw257.

Sammons, M. A., Nguyen, T.-A. T., McDade, S. S., and Fischer, M. (2020). Tumor suppressor p53: from engaging DNA to target gene regulation. *Nucleic Acids Res.* 48, 8848–8869. doi: 10.1093/nar/gkaa666.

Shieh, S.-Y., Ikeda, M., Taya, Y., and Prives, C. (1997). DNA Damage-Induced Phosphorylation of p53 Alleviates Inhibition by MDM2. *Cell* 91, 325–334. doi: 10.1016/S0092-8674(00)80416-X.

Siu, F., Bain, P. J., LeBlanc-Chaffin, R., Chen, H., and Kilberg, M. S. (2002). ATF4 is a mediator of the nutrient-sensing response pathway that activates the human asparagine synthetase gene. *J. Biol. Chem.* 277, 24120–24127. doi: 10.1074/jbc.M201959200.

Skene, P. J., and Henikoff, S. (2017). An efficient targeted nuclease strategy for high-resolution mapping of DNA binding sites. *eLife* 6, e21856. doi: 10.7554/eLife.21856.

Smeenk, L., van Heeringen, S. J., Koeppel, M., van Driel, M. A., Bartels, S. J. J., Akkers, R. C., et al. (2008). Characterization of genome-wide p53-binding sites upon stress response. *Nucleic Acids Res.* 36, 3639–3654. doi: 10.1093/nar/gkn232.

Smith, R. P., Taher, L., Patwardhan, R. P., Kim, M. J., Inoue, F., Shendure, J., et al. (2013). Massively parallel decoding of mammalian regulatory sequences supports a flexible organizational model. *Nat. Genet.* 45, 1021–1028. doi: 10.1038/ng.2713.

Soneson, C., Love, M. I., and Robinson, M. D. (2015). Differential analyses for RNA-seq: transcript-level estimates improve gene-level inferences. *F1000Research* 4, 1521. doi: 10.12688/f1000research.7563.1.

Szak, S. T., Mays, D., and Pietenpol, J. A. (2001). Kinetics of p53 binding to promoter sites in vivo. *Mol. Cell. Biol.* 21, 3375–3386. doi: 10.1128/MCB.21.10.3375-3386.2001.

Tameire, F., Verginadis, I. I., Leli, N. M., Polte, C., Conn, C. S., Ojha, R., et al. (2019). ATF4 couples MYC-dependent translational activity to bioenergetic demands during tumour progression. *Nat. Cell Biol.* 21, 889–899. doi: 10.1038/s41556-019-0347-9.

Taniuchi, S., Miyake, M., Tsugawa, K., Oyadomari, M., and Oyadomari, S. (2016). Integrated stress response of vertebrates is regulated by four eIF2α kinases. *Sci. Rep.* 6, 32886. doi: 10.1038/srep32886.

Thakore, P. I., D'Ippolito, A. M., Song, L., Safi, A., Shivakumar, N. K., Kabadi, A. M., et al. (2015). Highly specific epigenome editing by CRISPR-Cas9 repressors for silencing of distal regulatory elements. *Nat. Methods* 12, 1143–1149. doi: 10.1038/nmeth.3630.

Tian, X., Ahsan, N., Lulla, A., Lev, A., Abbosh, P., Dicker, D. T., et al. (2021). P53-independent

partial restoration of the p53 pathway in tumors with mutated p53 through ATF4 transcriptional modulation by ERK1/2 and CDK9. *Neoplasia* 23, 304–325. doi: 10.1016/j.neo.2021.01.004.

van Maanen, J. M. S., Retel, J., de Vries, J., and Pinedo, H. M. (1988). Mechanism of Action of Antitumor Drug Etoposide: A Review. *JNCI J. Natl. Cancer Inst.* 80, 1526–1533. doi: 10.1093/jnci/80.19.1526.

Vassilev, L. T., Vu, B. T., Graves, B., Carvajal, D., Podlaski, F., Filipovic, Z., et al. (2004). In Vivo Activation of the p53 Pathway by Small-Molecule Antagonists of MDM2. *Science* 303, 844–848. doi: 10.1126/science.1092472.

Vattem, K. M., and Wek, R. C. (2004). Reinitiation involving upstream ORFs regulates ATF4 mRNA translation in mammalian cells. *Proc. Natl. Acad. Sci. U. S. A.* 101, 11269–11274. doi: 10.1073/pnas.0400541101.

Verfaillie, A., Svetlichnyy, D., Imrichova, H., Davie, K., Fiers, M., Atak, Z. K., et al. (2016). Multiplex enhancer-reporter assays uncover unsophisticated TP53 enhancer logic. *Genome Res.* 26, 882–895. doi: 10.1101/gr.204149.116.

Vihervaara, A., Duarte, F. M., and Lis, J. T. (2018). Molecular mechanisms driving transcriptional stress responses. *Nat. Rev. Genet.* 19, 385–397. doi: 10.1038/s41576-018-0001-6.

Weidenfeld-Baranboim, K., Hasin, T., Darlyuk, I., Heinrich, R., Elhanani, O., Pan, J., et al. (2009). The ubiquitously expressed bZIP inhibitor, JDP2, suppresses the transcription of its homologue immediate early gene counterpart, ATF3. *Nucleic Acids Res.* 37, 2194–2203. doi: 10.1093/nar/gkp083.

Xie, Z., Bailey, A., Kuleshov, M. V., Clarke, D. J. B., Evangelista, J. E., Jenkins, S. L., et al. (2021). Gene Set Knowledge Discovery with Enrichr. *Curr. Protoc.* 1. doi: 10.1002/cpz1.90.

Yeo, N. C., Chavez, A., Lance-Byrne, A., Chan, Y., Menn, D., Milanova, D., et al. (2018). An enhanced CRISPR repressor for targeted mammalian gene regulation. *Nat. Methods* 15, 611–616. doi: 10.1038/s41592-018-0048-5.

Younger, S. T., and Rinn, J. L. (2017). p53 regulates enhancer accessibility and activity in response to DNA damage. *Nucleic Acids Res.* 45, 9889–9900. doi: 10.1093/nar/gkx577.

Yu, X., Vazquez, A., Levine, A. J., and Carpizo, D. R. (2012). Allele-Specific p53 Mutant Reactivation. *Cancer Cell* 21, 614–625. doi: 10.1016/j.ccr.2012.03.042.

Zaccara, S., Tebaldi, T., Pederiva, C., Ciribilli, Y., Bisio, A., and Inga, A. (2014). p53-directed translational control can shape and expand the universe of p53 target genes. *Cell Death Differ.* 21, 1522–1534. doi: 10.1038/cdd.2014.79.

Zeitlinger, J. (2020). Seven myths of how transcription factors read the cis-regulatory code. *Curr. Opin. Syst. Biol.* 23, 22–31. doi: 10.1016/j.coisb.2020.08.002.

Zeron-Medina, J., Wang, X., Repapi, E., Campbell, M. R., Su, D., Castro-Giner, F., et al. (2013). A polymorphic p53 response element in KIT ligand influences cancer risk and has undergone natural selection. *Cell* 155, 410–22. doi: 10.1016/j.cell.2013.09.017.

Zhan, Q., Bae, I., Kastan, M. B., and Fornace, A. J. (1994). The p53-dependent gamma-ray response of GADD45. *Cancer Res.* 54, 2755–2760.

Zhan, Q., Chen, I.-T., Antinore, M. J., and Albert J. Fornace, J. (1998). Tumor Suppressor p53 Can Participate in Transcriptional Induction of the GADD45 Promoter in the Absence of Direct DNA Binding. *Mol. Cell. Biol.* 18, 2768. doi: 10.1128/mcb.18.5.2768.

Zhang, S., Zhou, L., Hong, B., van den Heuvel, A. P. J., Prabhu, V. V., Warfel, N. A., et al. (2015). Small-Molecule NSC59984 Restores p53 Pathway Signaling and Antitumor Effects against Colorectal Cancer via p73 Activation and Degradation of Mutant p53. *Cancer Res.* 75, 3842–3852. doi: 10.1158/0008-5472.CAN-13-1079.

Zhang, Y., and Dong, C. (2007). Regulatory mechanisms of mitogen-activated kinase signaling. *Cell. Mol. Life Sci.* 64, 2771–2789. doi: 10.1007/s00018-007-7012-3.

Zhang, Y., Liu, T., Meyer, C. A., Eeckhoute, J., Johnson, D. S., Bernstein, B. E., et al. (2008). Model-based analysis of ChIP-Seq (MACS). *Genome Biol.* 9, R137. doi: 10.1186/gb-2008-9-9-r137.

Zhu, J., Sammons, M. A., Donahue, G., Dou, Z., Vedadi, M., Getlik, M., et al. (2015). Gain-of-function p53 mutants co-opt chromatin pathways to drive cancer growth. *Nature* 525, 206–211. doi: 10.1038/nature15251.

FIGURE 1

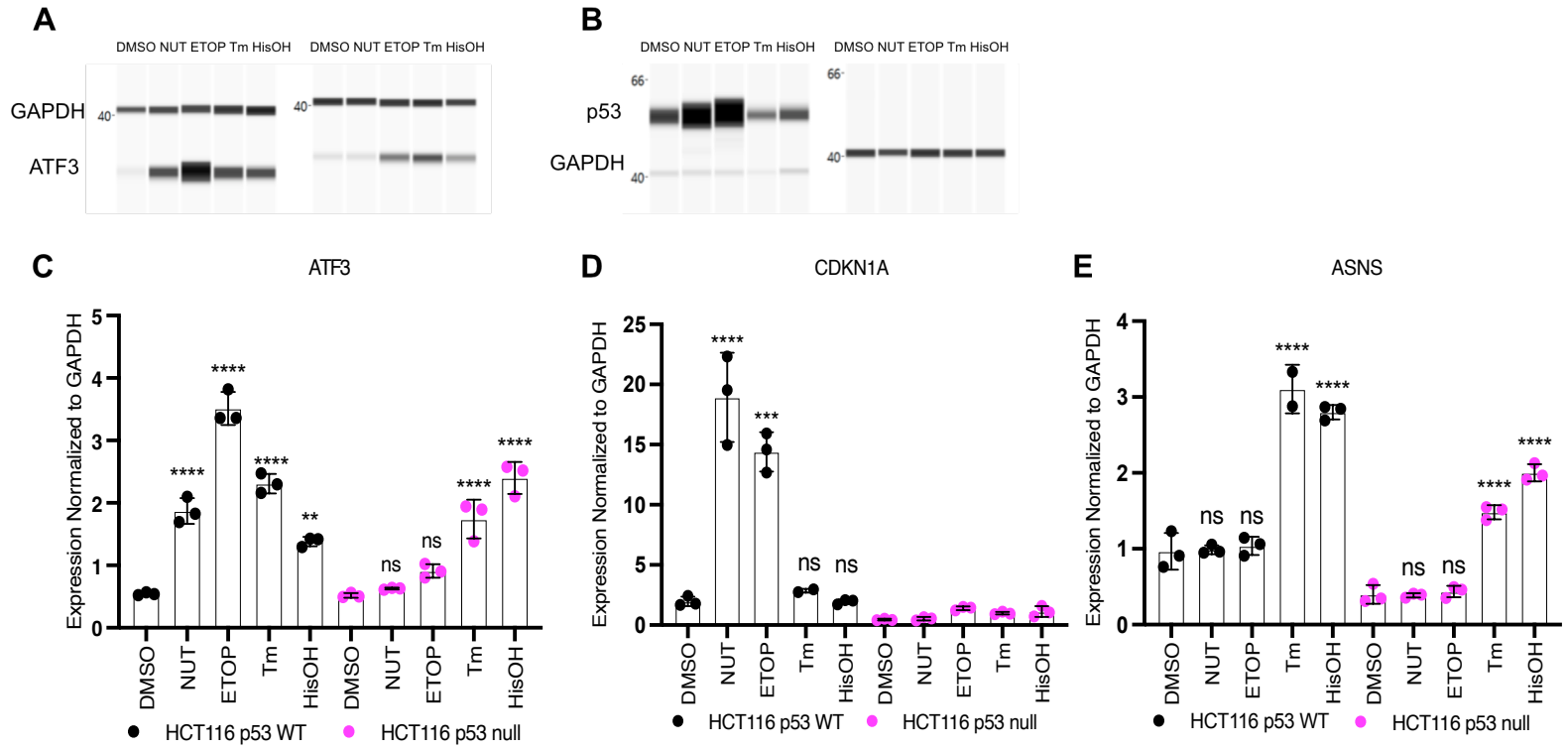

FIGURE 2

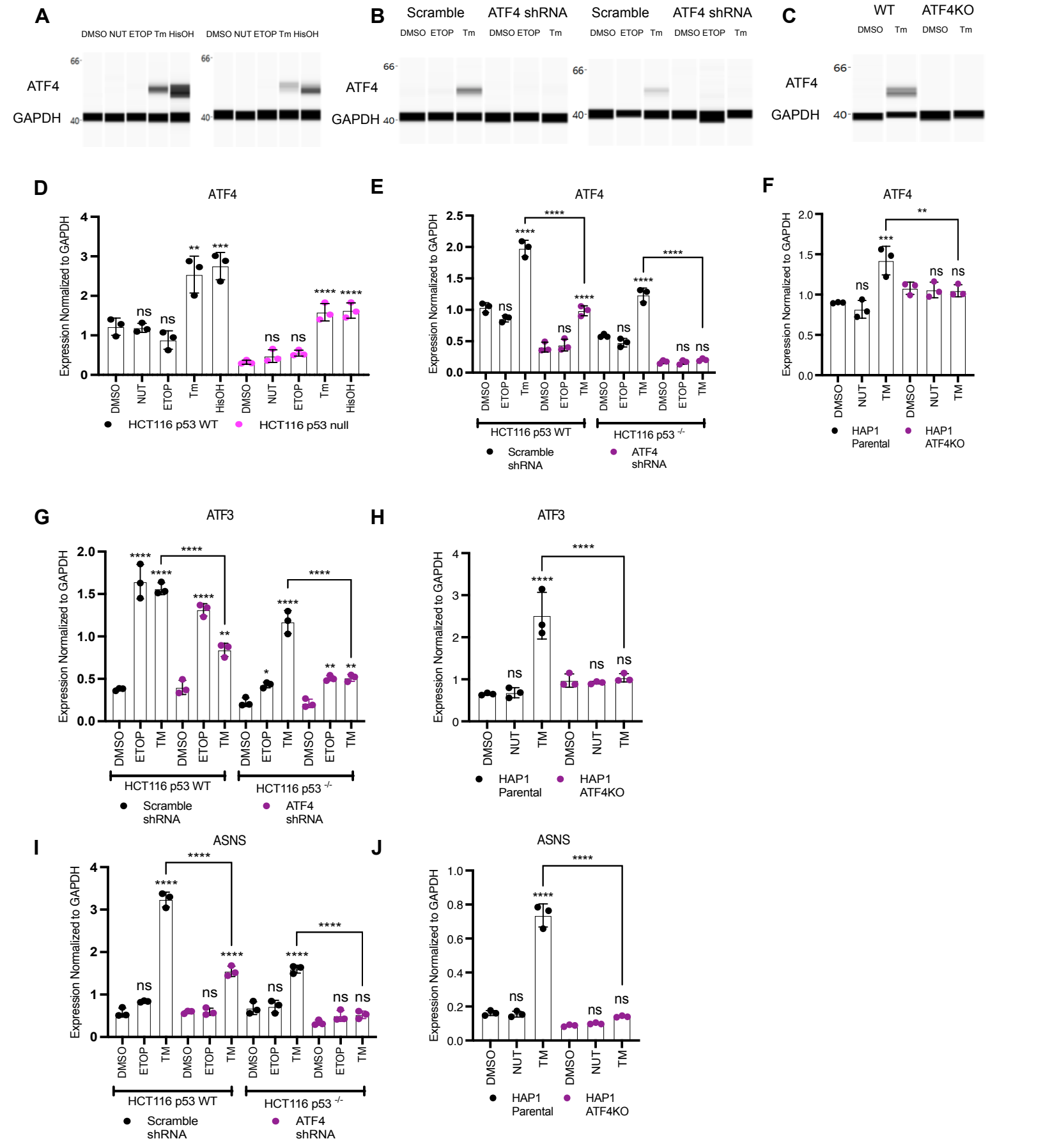

FIGURE 3

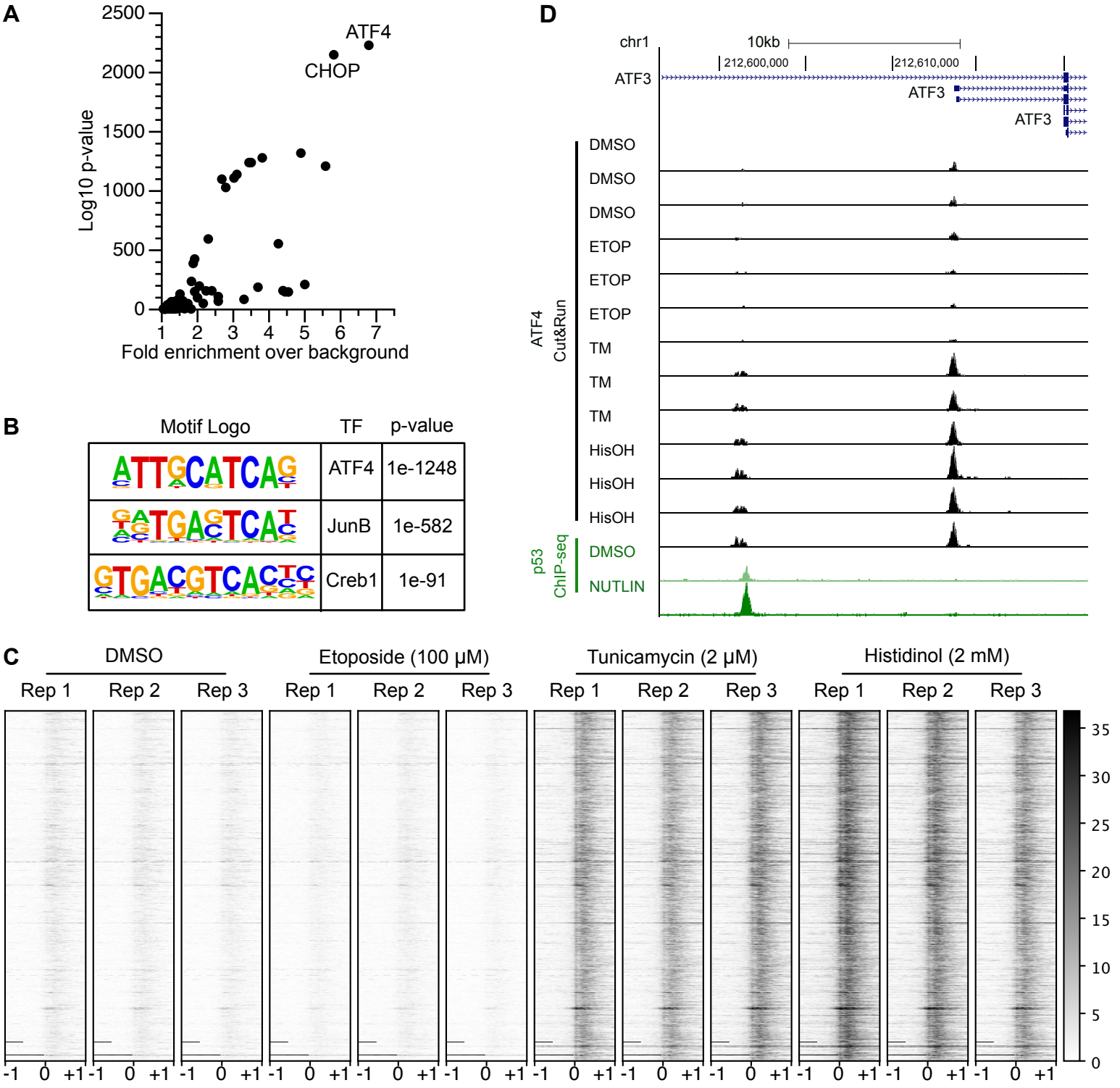

FIGURE 4

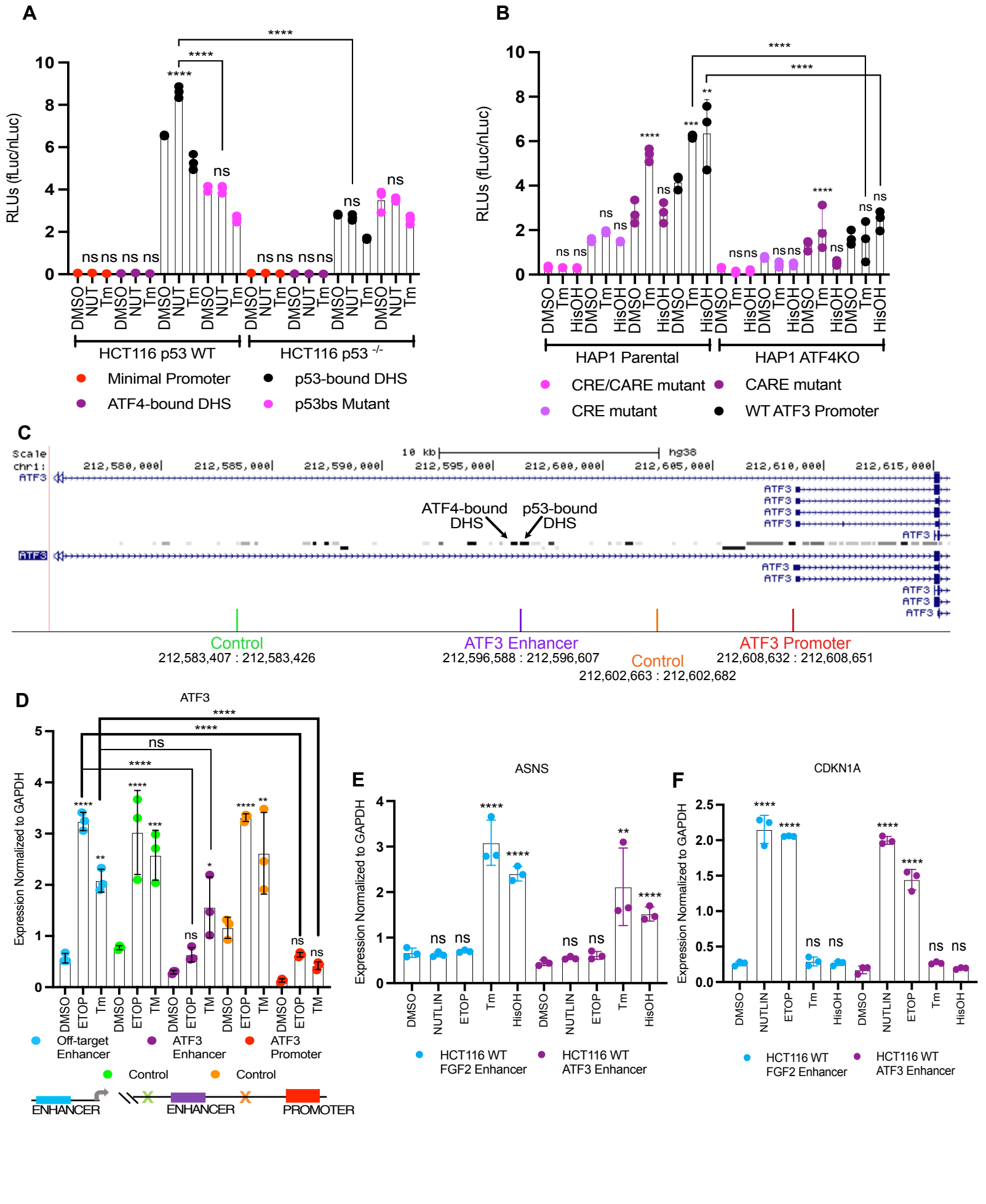

FIGURE 5

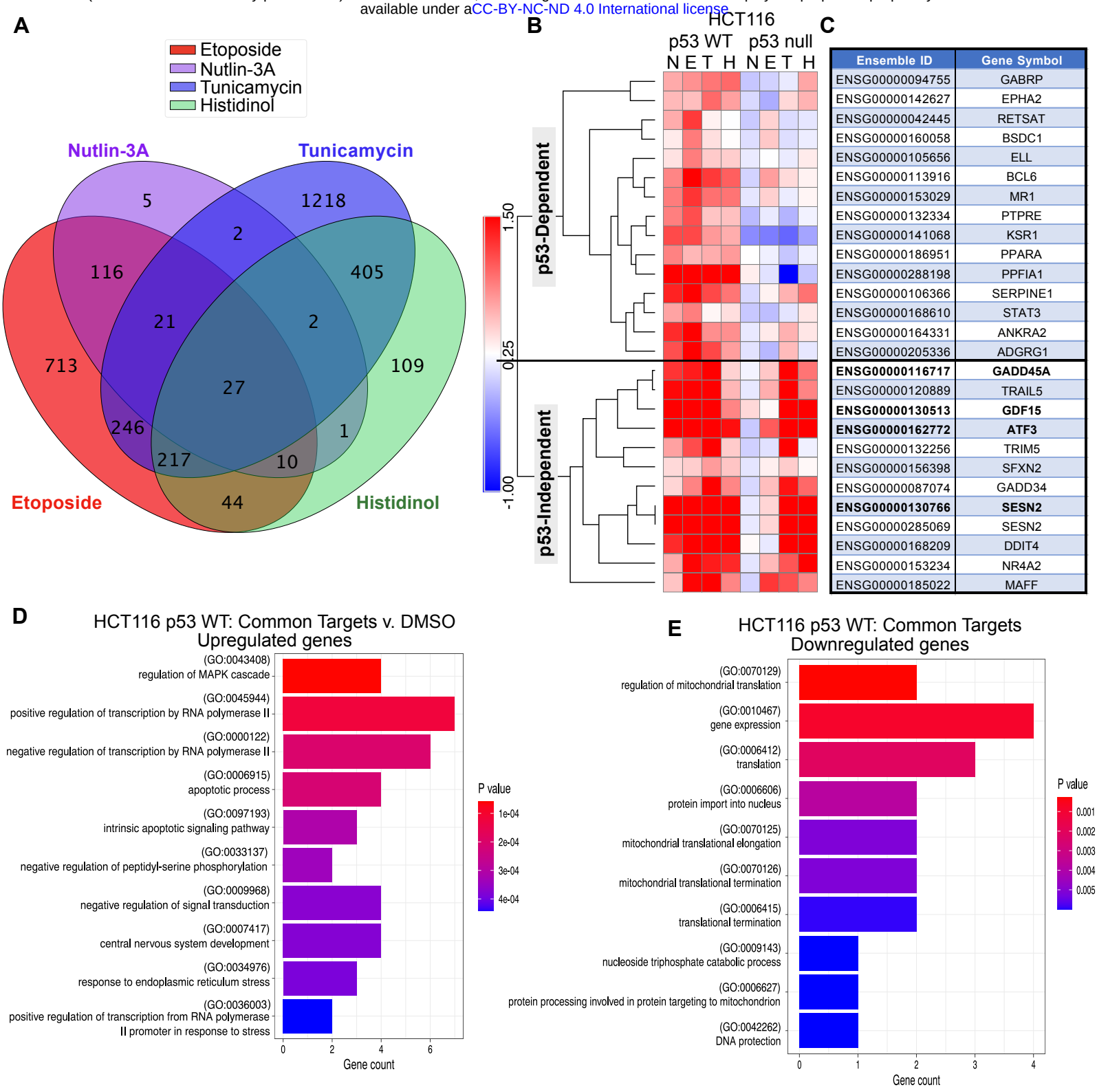

Ensemble ID	Gene Symbol
ENSG00000094755	GABRP
ENSG00000142627	EPHA2
ENSG00000042445	RETSAT
ENSG00000160058	BSDC1
ENSG00000105656	ELL
ENSG00000113916	BCL6
ENSG00000153029	MR1
ENSG00000132334	PTPRE
ENSG00000141068	KSR1
ENSG00000186951	PPARA
ENSG00000288198	PPFIA1
ENSG00000106366	SERPINE1
ENSG00000168610	STAT3
ENSG00000164331	ANKRA2
ENSG00000205336	ADGRG1
ENSG00000116717	**GADD45A**
ENSG00000120889	TRAIL5
ENSG00000130513	**GDF15**
ENSG00000162772	**ATF3**
ENSG00000132256	TRIM5
ENSG00000156398	SFXN2
ENSG00000087074	GADD34
ENSG00000130766	**SESN2**
ENSG00000285069	SESN2
ENSG00000168209	DDIT4
ENSG00000153234	NR4A2
ENSG00000185022	MAFF

FIGURE 6

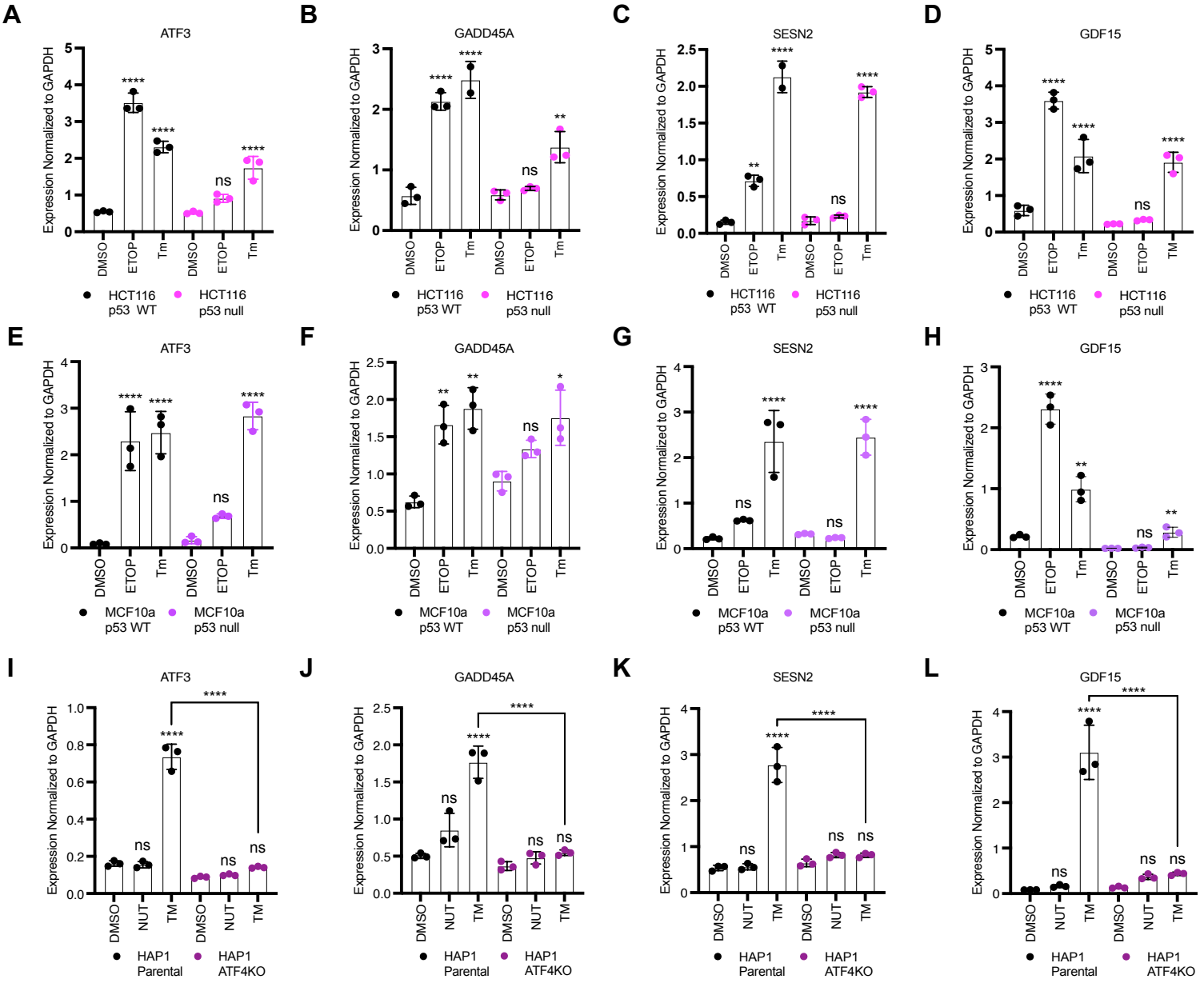

FIGURE 7

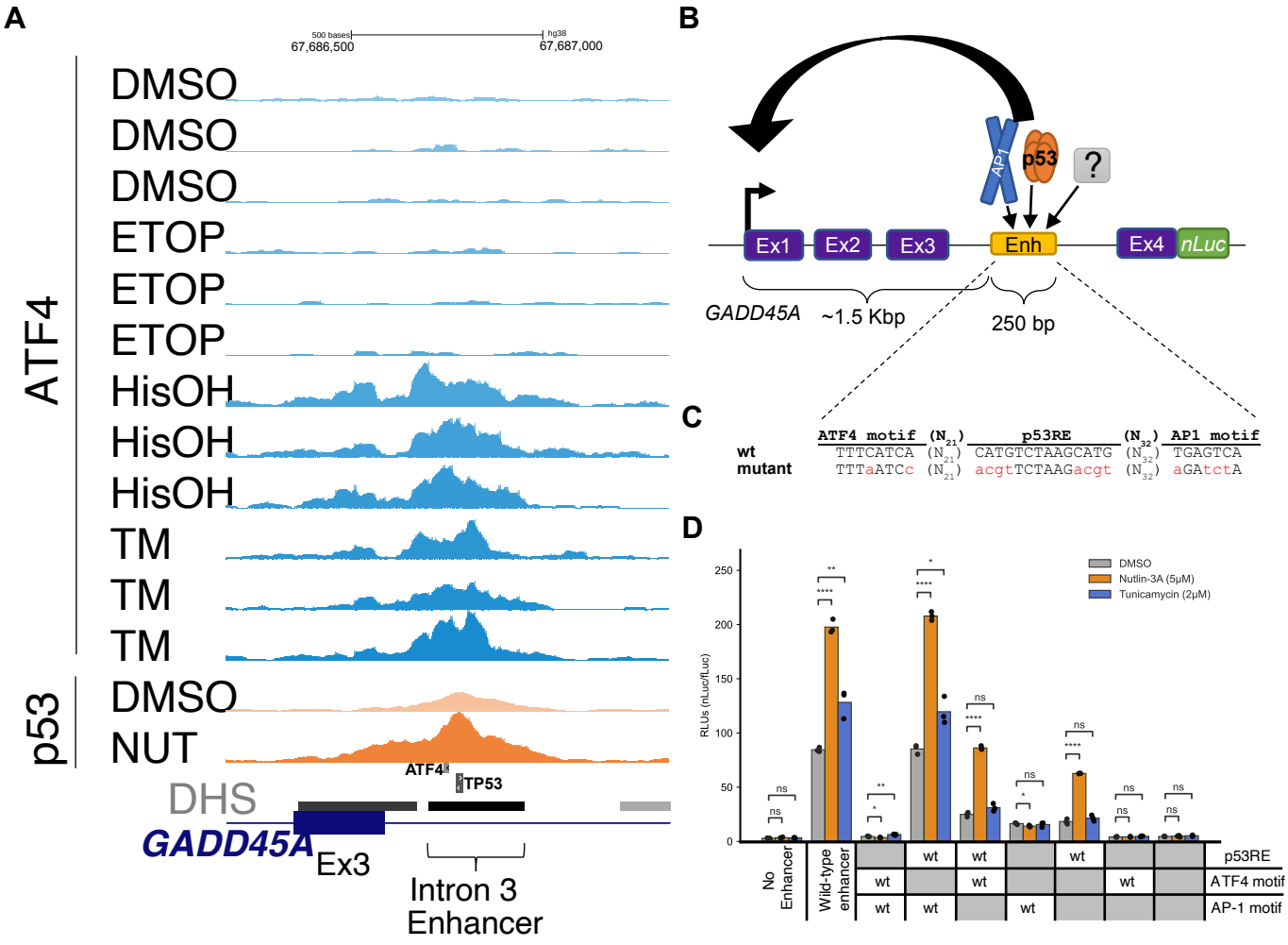
A
500 bases
hg38
67,686,500
67,687,000
ATF4
DMSO
DMSO
DMSO
ETOP
ETOP
ETOP
HisOH
HisOH
HisOH
TM
TM
TM
p53
DMSO
NUT
ATF4
TP53
DHS
GADD45A
Ex3
Intron 3
Enhancer
B
AP-1
p53
?
Ex1
Ex2
Ex3
Enh
Ex4
nLuc
GADD45A
~1.5 Kbp
250 bp
C
ATF4 motif (N21) p53RE (N32) AP1 motif
wt TTTCATCA (N21) CATGTCTAAGCATG (N32) TGAGTCA
mutant TTTaATCc (N21) acgtTCTAAGacgt (N32) aGAtctA
D
DMSO
Nutlin-3A (5μM)
Tunicamycin (2μM)
RLUs (nLuc/fLuc)
250
200
150
100
50
0
ns
*
**
****
No Enhancer
Wild-type enhancer
p53RE
ATF4 motif
AP-1 motif
wt

FIGURE 8

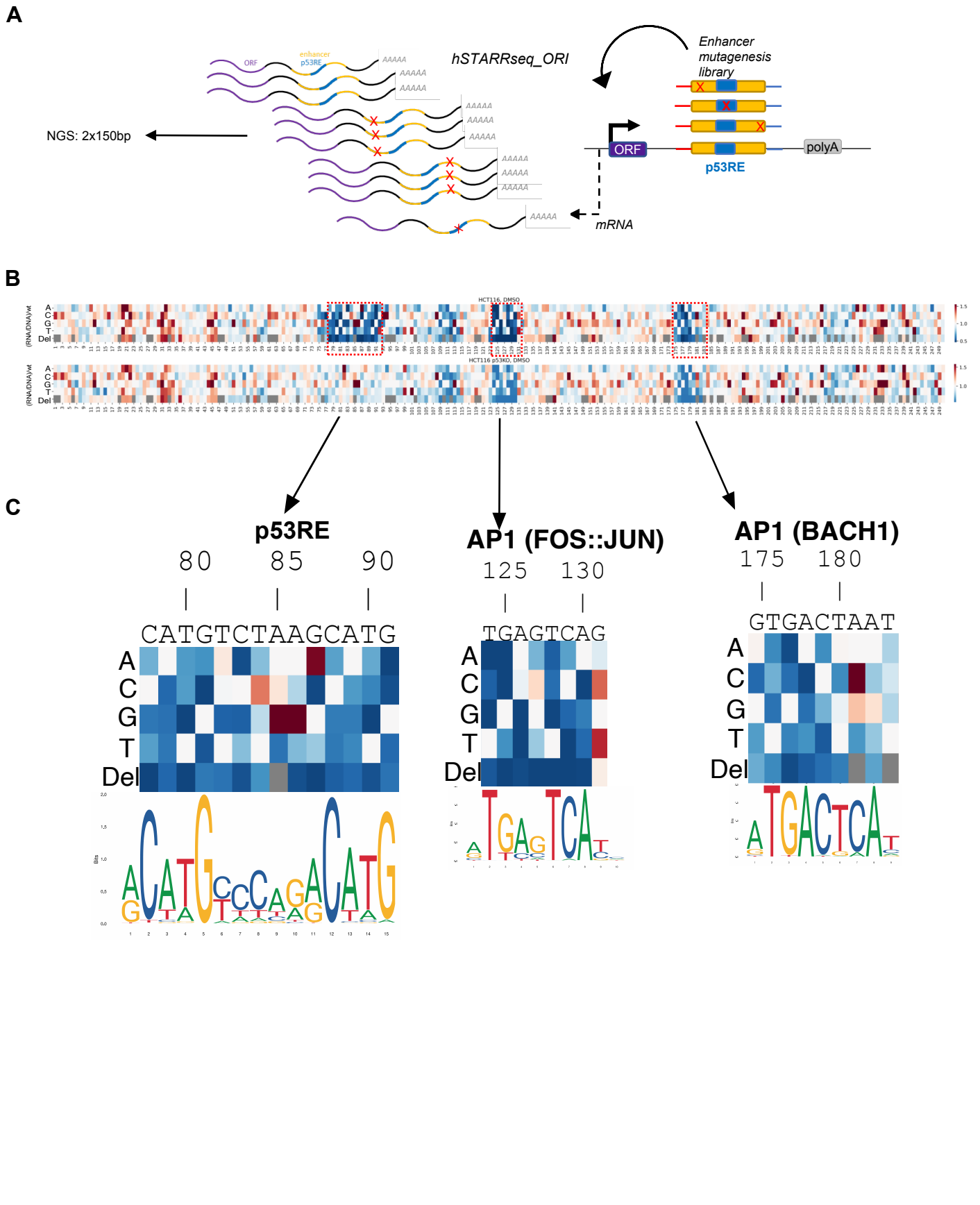
A
ORF
enhancer
p53RE
AAAAA
hSTARRseq_ORI
NGS: 2x150bp
Enhancer
mutagenesis
library
ORF
polyA
p53RE
mRNA
B
HCT116_DMSO
HCT116_p53RE_DMSO
(RNA/DNA)/wt
A
C
G
T
Del
C
p53RE
80
85
90
CATGTCTAAGCATG
AP1 (FOS::JUN)
125
130
TGAGTCAG
AP1 (BACH1)
175
180
GTGACTAAT
Bits

FIGURE 9

A

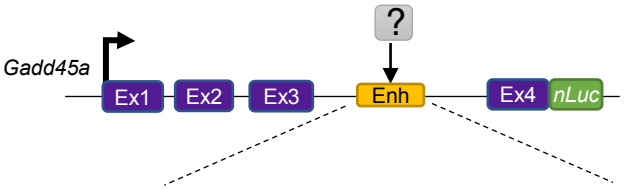

TF name	ETV6	AP1 (BACH1)	GLIS3/POU6F2
wt	AGCGGAAGAG (N_{58})	GTGACTAAT (N_{48})	CCCTCATTAAG
mut	AGCGGtgGAG (N_{58})	GTaACTcAT (N_{48})	CCgTCATaAAG
mut name	ETV6 (A112T) ETV6 (A113G)	BACH1 (G177A) BACH1 (A181C)	GLIS3 (C234G) POU6F2 (T239A)

B

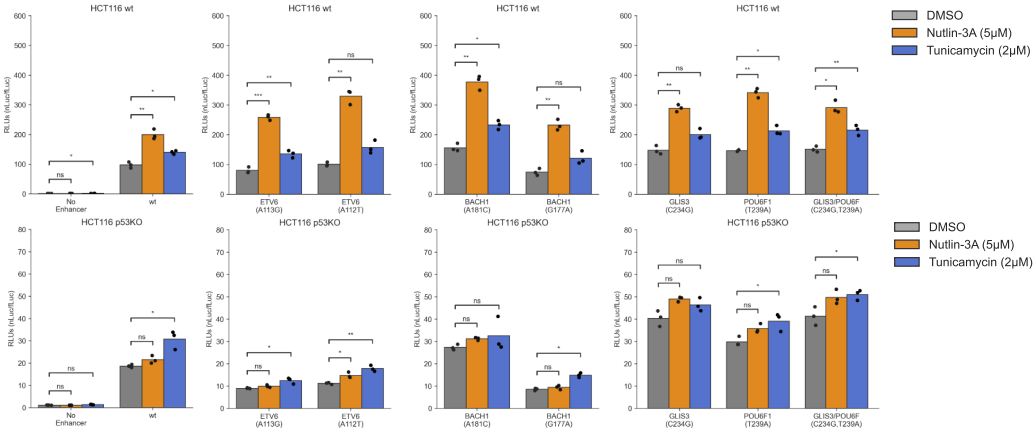

FIGURE S1

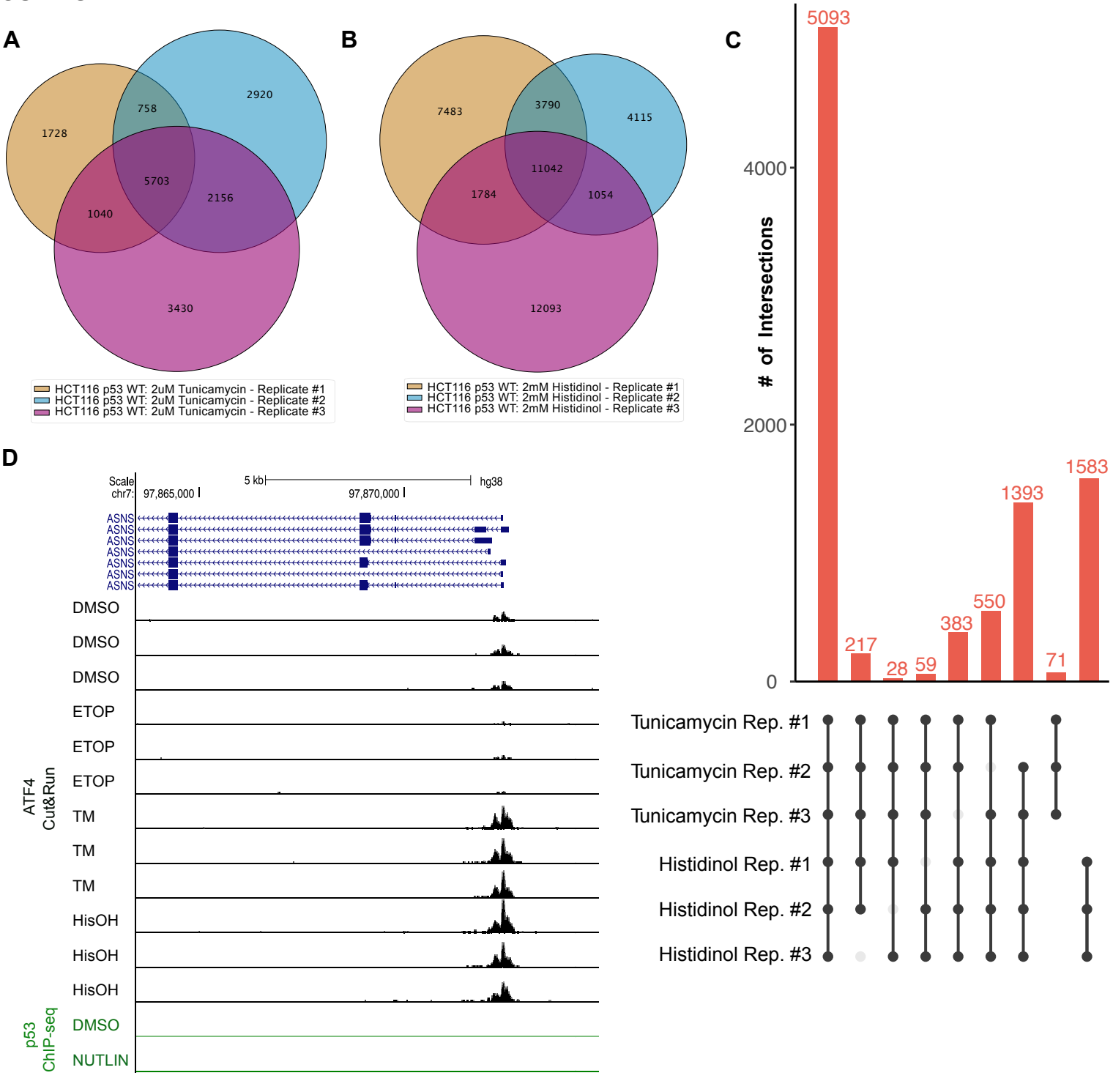

FIGURE S2

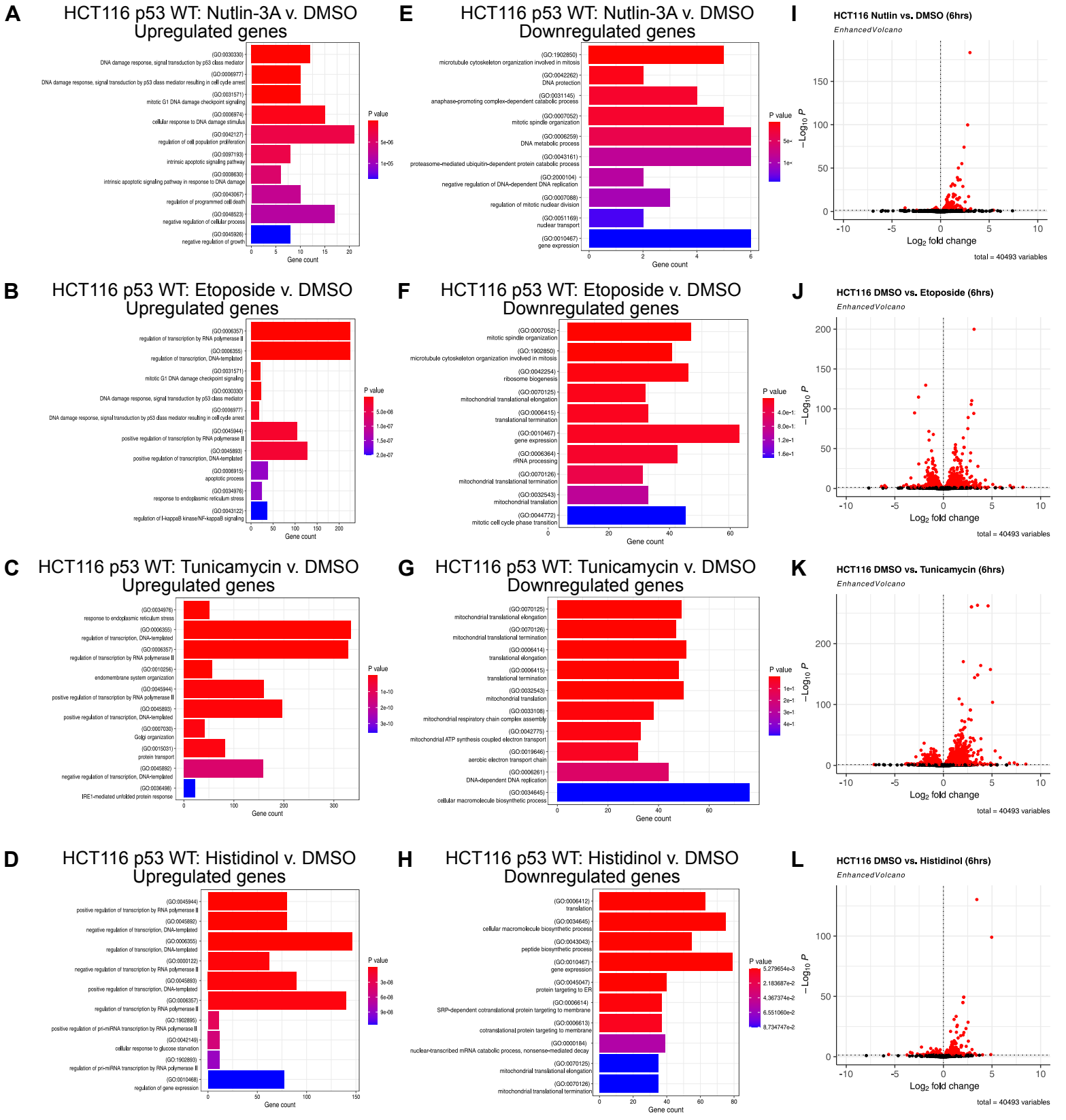

FIGURE 63

A

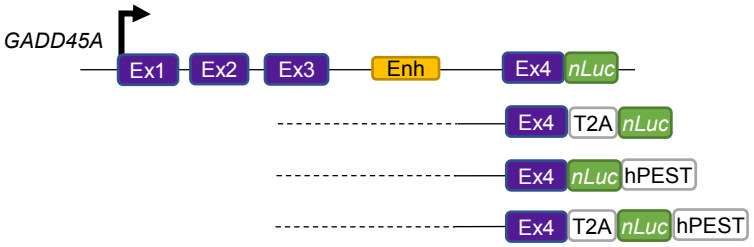
GADD45A
Ex1
Ex2
Ex3
Enh
Ex4
nLuc
Ex4
T2A
nLuc
Ex4
nLuc
hPEST
Ex4
T2A
nLuc
hPEST

B

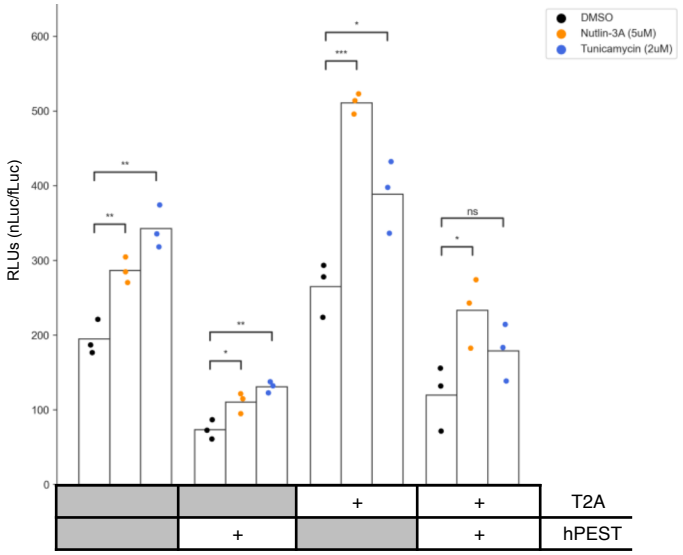
DMSO
Nutlin-3A (5uM)
Tunicamycin (2uM)
RLUs (nLuc/fLuc)
600
500
400
300
200
100
0
**
**
*
**
*
***
ns
*
+
+
T2A
+
+
hPEST

FIGURE S4

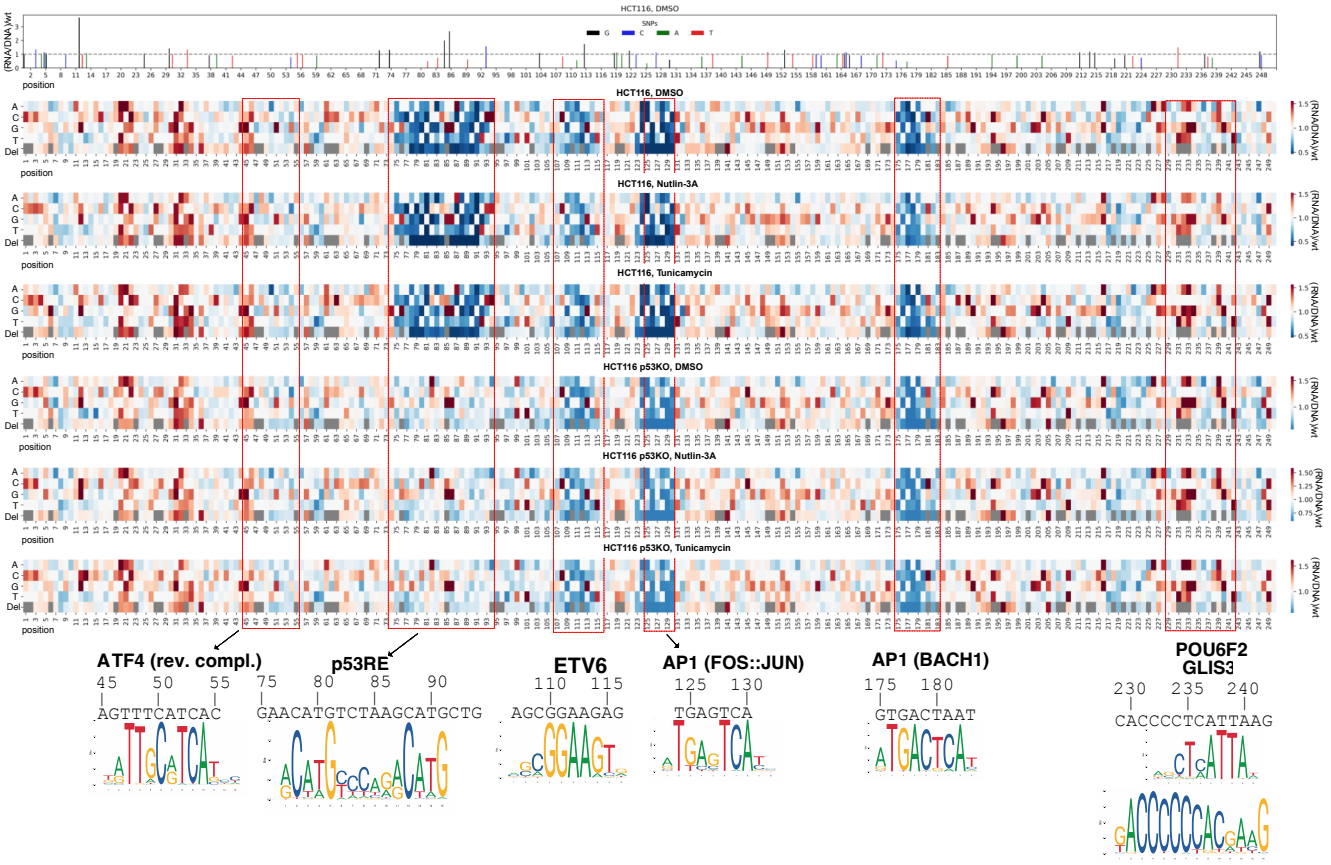
HCT116, DMSO
SNPs
(RNA/DNA).wt
position
HCT116, DMSO
HCT116, Nutlin-3A
HCT116, Tunicamycin
HCT116 p53KO, DMSO
HCT116 p53KO, Nutlin-3A
HCT116 p53KO, Tunicamycin
ATF4 (rev. compl.)
p53RE
ETV6
AP1 (FOS::JUN)
AP1 (BACH1)
POU6F2
GLIS3